Lawrence Berkeley National Laboratory
Recent Work

Title
APPLICATION OF NOVEL NMR TECHNIQUES TO SOLIDS and LIQUID CRYSTALS

Permalink
https://escholarship.org/uc/item/7pp3g5sz

Author
Pines, Alexander.

Publication Date
1975-08-01

eScholarship.org Powered by the California Digital Library
University of California

0 0 0 0 4 5 0 5 7 4 5

Presented at the 2nd Specialized Colloque
Ampere, Budapest, Hungary,
August 25 - 29, 1975

RECEIVED
DEC 3 1975
LIBRARY AND
DOCUMENTS SECTION

LBL-4505

APPLICATION OF NOVEL NMR TECHNIQUES TO SOLIDS AND LIQUID CRYSTALS

Alexander Pines

August 1975

Prepared for the U. S. Energy Research and
Development Administration under Contract W-7405-ENG-48

For Reference

Not to be taken from this room

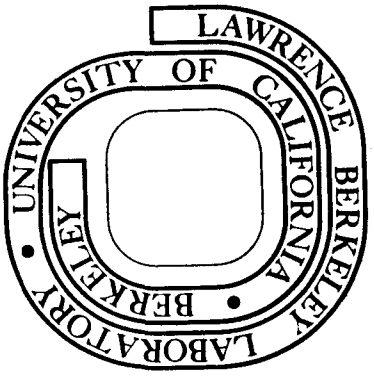

LBL-4505

DISCLAIMER

This document was prepared as an account of work sponsored by the United States Government. While this document is believed to contain correct information, neither the United States Government nor any agency thereof, nor the Regents of the University of California, nor any of their employees, makes any warranty, express or implied, or assumes any legal responsibility for the accuracy, completeness, or usefulness of any information, apparatus, product, or process disclosed, or represents that its use would not infringe privately owned rights. Reference herein to any specific commercial product, process, or service by its trade name, trademark, manufacturer, or otherwise, does not necessarily constitute or imply its endorsement, recommendation, or favoring by the United States Government or any agency thereof, or the Regents of the University of California. The views and opinions of authors expressed herein do not necessarily state or reflect those of the United States Government or any agency thereof or the Regents of the University of California.

0 0 0 0 4 4 0 6 7 4 6

Application of Novel NMR Techniques to Solids and Liquid Crystals*

Alexander Pines†

Department of Chemistry, University of California
and Materials and Molecular Research Division, Lawrence Berkeley Laboratory
Berkeley, California 94720

ABSTRACT

Techniques for obtaining high resolution nmr spectra of ^{13}C and ^{1}H in ordered phases are described. The latter involves double quantum transitions of the deuterium nuclear spins. Some simple quantitative aspects of these double-quantum processes are discussed. Applications of ^{13}C to hydrogen-bonding in solids and ordering in a nematic liquid crystal are shown and the effects on lineshapes of the ^{13}C resonance due to various kinds of molecular motion in solids and liquid crystals are described. In particular, some weak singularities in the powder spectrum for six-fold motion predicted by Baram, Luz, and Alexander, are computed numerically and verified experimentally. Finally, the first determination of the proton chemical shielding tensor in ice by solid state deuterium decoupling is reported and the proton lineshapes obtained between - 90°C and - 5°C in heavy ice are interpreted in terms of proton jumps in a potential with tetrahedral symmetry by motion of defects.

---

* Presented at the Second Specialized Colloque Ampere, Budapest, Hungary August, 1975.

† Alfred P. Sloan Fellow. On leave during Fall, 1975, at the Isotope Department, Weizmann Institute of Science, Rehovot, Israel, and Department of Physics, University of Dortmund, West Germany.

0 0 0 0 4 4 0 6 7 4 7

I. INTRODUCTION

It is a great privilege to be able to lecture at an international conference here in Budapest. I am grateful for the opportunity to describe to you some of our work on nmr of solids and liquid crystals and to present to you some of the recent results obtained with my colleagues and collaborators.

Rather than concentrate in great detail on one narrow item, I shall attempt to describe briefly some examples from a class of experiments aimed at elucidating the microscopic structure and molecular dynamics of solids and liquid crystals using nmr. This is intended to indicate what is involved in the techniques employed and the scope of applicability of nmr for such microscopic studies in ordered phases.

Before I begin, permit me to mention the people with whom this research was and is being done. Much of the work on spin dynamics, decoupling and applications to solids, involves collaboration with Professor M. Mehring of the Physics Department, University of Dortmund, West Germany. Professor Mehring is presenting some details of the spin dynamics research in another paper at this conference.[1] My colleagues in my laboratory at Berkeley involved in various aspects of this research are Dr. David J. Ruben, Dr. Shimon Vega, Dr. Alfred Höhener, Mr. Tom W. Shattuck, Mr. Stuart A. Allison and Mr. David E. Wemmer.

It is well known that nmr is an excellent tool for the study of molecular structure and dynamics. Its application to ordered

phases such as solids and liquid crystals, however, is not so straightforward. The reason is that the magnetic dipolar coupling between nuclei does not average to zero as in isotropic fluids and gives rise to broad, featureless spectra. When I was a student with Professor Waugh, we developed an extremely simple (in principle) way out of this which was applied primarily to ^{13}C in natural abundance ($\sim$ 1%) in solids.[2] The technique involves strong spin-decoupling of the abundant proton from the ^{13}C nuclei giving rise to sharp spectra and resolution of chemical shifts in solids. The low sensitivity of ^{13}C resonance was enhanced by transferring polarization from the protons using ideas developed by Hartmann and Hahn in Berkeley.

In the next section I shall show some of our first novel applications of these techniques to molecular dynamics in solids and liquid crystals. Some ingenious recent developments of Professor Waugh and his group have now opened the way to obtaining high resolution <u>dipolar</u> spectra of rare nuclei[3] and I hope that he will be describing these in his paper at this conference. I shall not dwell at all on this subject, but spend part of the time on our applications, to demonstrate that the expected fruitfulness of the techniques has indeed been borne out. The examples I have chosen to present include the effects of molecular ordering on high resolution lineshapes in liquid crystals and their effect of the symmetry of potential barriers to molecular motion in solids on high-resolution powder lineshapes.[4]

0 0 0 0 4 4 0 6 7 4 8

Regarding the other part of the talk, it has certainly occurred to you that ^{13}C (as well as other rare nuclear isotopes) is not the only nucleus of interest in organic solids and liquid crystals. The best example of an important abundant nucleus is the proton, ^{1}H. To date, the only successful approach to high resolution nmr of protons in solids has been the multiple-pulse techniques of Haeberlen and Waugh.[5] These are technically quite difficult and because of this applications have not been widespread.

An appealing idea would be to dilute the protons, say in a bath of deuterium; the protons could then be regarded as rare nuclei and high resolution nmr spectra obtained by spin-decoupling of the deuterium. This has been used for ordered solutes in liquid crystals, for example by Meiboom et al.[6] and by Emsley et al.[7] At first glance this appears to be an immensely difficult task, as shown in the next section, since the nuclear quadrupole splitting of deuterium nuclei is about 200 kHz. If we compare this with the small splittings ($\sim$ 3 kHz) for the molecules dissolved in liquid crystals, we see that about $(200/3)^2 \sim 4000$ times more rf power would be needed to decouple in solids and the liquid crystal molecules themselves. Since the Meiboom and Emsley groups already complain about the power required for their experiments, the whole idea seems quite preposterous unless we are willing to accept the melting of our probes as a routine matter.

Fortunately, as indicated already by Snyder and Meiboom,[6] we are saved by a phenomenon as simple as double-quantum transitions of the deuterium nuclei, which make the decoupling problem much

simpler than it might otherwise seem. Thus, we have investigated this idea theoretically and, although still not technically trivial, we have applied it successfully in solids to several problems including the first high resolution nmr spectrum of residual protons in deuterated materials,[8] and have studied the dynamics of proton motion in heavy ice. We have also looked at a number of organic solids. This approach should form a useful alternative and extension to multiple-pulse nmr of proton in ordered phases, in particular for application to larger molecules where deuterium and proton isotopic labelling can be used, or where normal proton T_2's are extremely short.

0 0 0 0 4 4 0 6 7 4 9

II. TECHNIQUES

A. ^{13}C - ^{1}H Double-Resonance

The basic premise for the high resolution nmr of rare nuclei[4] in the presence of abundant nuclei (I), exluding any sensitivity enhancement, is extremely simple as depicted in Fig. 1. What is the output which we require from the technique? Well, since we are interested in the orientational effects of molecular motion, we require something which is sensitive to orientation. In the case of ^{13}C, this is provided by the chemical shielding tensor. An example of the directional properties of the ^{13}C tensor for a common functional group, the carboxyl group, determined by single crystal techniques[9] is shown in Fig. 2. We have obtained such tensors for a variety of functional groups; it is this information which we use in the microscopic studies, since clearly different modes of motion will involve different linear combinations of the principal elements of the tensor.

Note that the tensor depicted is for an isolated, symmetric (C_{2v}) carboxyl group. Any deviations from this symmetry caused by hydrogen-bonding, as shown in Fig. 3, may cause different orientations of the principal axes.[10] This is illustrated with some selected examples in Table 1 showing carboxyl ^{13}C shielding tensors which we have determined for various groups with unequal CO bond lengths.

In any case, the technical aspect of ^{13}C - ^{1}H double resonance for obtaining high resolution, ^{13}C spectra seems to be solved and is now well into the stage of applications, as the next sections, and other papers at this conference, will show.

B. $^2H - {}^1H$ Double-Resonance[8]

The nature of the problem in the case of deuterium decoupling in solids is shown in Figure 4. Let us apply an irradiating field of intensity ω_1 at the centre of the deuterium resonance. Since the amount we are off resonance ($\Delta\omega$) from the allowed deuterium transitions, is, on the average:

$$\Delta\omega \sim Q \tag{1}$$

the criterion for effective spin decoupling (through the allowed transitions) is given by

$$P_{-1,0} \sim \omega_1{}^2 \sim Q^2 \tag{2}$$

where P_{ij} are transition probabilities between levels i and j. This is a prohibitive requirement on ω_1 if Q is large, and comes about since we need to "spread" the irradiating field over the whole range of deuterium absorption. I believe it is for this reason that no one has attempted this approach in solids.

Let us look, now, at the possibility for a "forbidden" deuterium transition from m = -1 to m = +1 using only the back of a small envelope. Let us look at Fig. 5(a) which depicts the allowed transitions of ω_A and ω_B and the transition from -1 to +1 as a <u>double-quantum transition</u> at ω_0. To calculate the effectiveness of decoupling by this transition we simply go to second order perturbation theory, yielding a criterion for narrowing of the proton lines:

0 0 0 0 4 4 0 6 7 5 0

$$P_{-1,+1} \sim \frac{\omega_1^4}{Q^2} \sim D^2$$

i.e.,

$$\omega_1^2 \sim QD \qquad (3)$$

which is clearly a weaker requirement on ω_1, since Q >> D. In fact, it is the decoupling induced by these double-quantum transitions which saves us and makes the approach technically feasible. The basic reason why this should work is that although the transition at ω_0 is a non-linear one (not really forbidden, except in first order), it is resonant for all the nuclei. A complete theory which will be published soon has been worked out by Dr. Vega for this problem and I shall not describe the details here. Figure 5(b) summarizes the qualitative arguments.

To see how this approach works, we show in Fig. 6 the line narrowing produced in a sample of deuterated (> 99%) dimethyl sulfoxide (DMSO) in the solid state. As shown in Fig. 7 the efficiency of the decoupling is extremely sensitive to the frequency of deuterium irradiation at low powers, similar to the behavior observed in the liquid crystal solutes.[6,7] This is one of the features which distinguishes the spin-decoupling by multiple-quantum transitions from that induced by normal first order processes, and is well accounted for by the theory.

Thus, high resolution proton nmr by deuterium decoupling in ordered phases appears to be solved and should provide a convenient alternative approach to this problem. Its main advantages are

technical simplicity and the possibility of isotopic labelling in large molecules. In addition, it extends the realm of applicability of multiple-pulse nmr by making it feasible to work with longer cycle times on partially deuterated materials. Its disadvantages are the synthetic requirement of deuteration, and the fact that substituting deuterium for protons may substantially affect the chemical and physical properties of the system.

C. Spectrometer[11]

Finally, to end this section, Fig. 8 shows the spectrometer used for both the ^{13}C - ^{1}H and ^{2}H - ^{1}H experiments, which operates at 185 MHz for ^{1}H. It uses a computer-controlled (Nova 820) pulse programmer, quadrature phase detection and homebuilt high-power rf amplifiers. The probe shown schematically in Fig. 9 is designed for the geometry of our superconducting solenoid, incorporating homebuilt high voltage capacitors, crystal goniometer, pulsed quadrupole gradient coils and feedback temperature control.

0 0 0 0 4 4 0 6 7 5 1

III. ILLUSTRATIVE APPLICATIONS

A. Effect of Liquid Crystal Phase Transitions

As a simple example of applying ^{13}C nmr to liquid crystals, I shall describe to you something which we have shown previously,[12] demonstrating the effects of molecular aggregation and motion on the spectra in the simplest liquid crystal phase transition, isotropic-nematic. This is introduced by Fig. 10, which shows the structure of a typical liquid crystal molecule, MBBA, and the orientation of the chemical shielding tensors for its two main functional groups, aromatic and aliphatic, as determined from single crystal studies.[13,14] In the isotropic phase, the chemical shift is given by the average of the tensor elements.

$$\sigma_i = \frac{1}{3} \mathrm{Tr}\, \sigma \qquad (4)$$

In the nematic phase, since the long molecular axis will be along the magnetic field on the average, Fig. 10 shows that the aromatic lines should shift downfield (since σ_{33} is perpendicular to the long axis) while the aliphatic lines should shift upfield (since σ_{33} is along the long axis). This is exactly what we observe as shown in Fig. 11, which shows "typical" (used, as usual, to mean unusually good) spectra in the isotropic and nematic phases of MBBA. Similar spectra have also been observed at high frequency recently by Clin.[15]

The shift in the nematic phase, assuming the molecules rotate rapidly and isotropically about their long axes is given by:

$$\sigma = \sigma_i + \frac{2}{3} S(\bar{\sigma}_{\parallel} - \bar{\sigma}_{\perp}) \qquad (5)$$

where S is the order parameter of the long molecular axis which fluctuates by θ away from the magnetic field.

$$S = \langle P_2 (\cos\theta) \rangle \qquad (6)$$

and $\bar{\sigma}_{\parallel}$ and $\bar{\sigma}_{\perp}$ are the averaged chemical shielding tensor elements relative to the long axis. Such data have been used to extract information in this phase and other liquid crystal phases about molecular order, conformational motion, effect of end chains on molecular ordering, spin-lattice relaxation and rotational order about the long axis.

B. Rotational Order in Smectic-C

In the liquid crystal smectic-C phase the molecules are organized in layers, with the long molecular axes tilted relative to the layer normals. This is depicted in Fig. 12a. As the sample is rotated, according to a model due to Luz and Meiboom[15] and Wise et al.[16], the different domains behave differently, minimizing their diamagnetic susceptibility anisotropy energy while maintaining a constant tilt angle, as depicted schematically in Fig. 12b. A theoretical model for the smectic-C phase has been proposed by McMillan[17] in which the molecular tilting is induced by transverse electric dipoles on the molecules, as shown in Fig. 13.

Since this model obviously requires a freezing of the molecular motion about the long axis in the smectic-C phase, much effort has been extended to examine this question experimentally, and has raised

0 0 0 0 4 4 0 6 7 5 2

some controversy. We have calculated the ^{13}C nmr lineshapes for the ortho aromatic carbons in p-octyloxyazoxybenzene (OAB), the analog of p-azoxyanisole (PAA) with 8-carbon chains[18] for models with various degrees of rotational freezing. Beginning with the general form of the Hamiltonian in the lab frame:

$$H = \sum_m (-1)^m F_{2m} T_{2-m} + \frac{1}{3} \mathrm{Tr}\, \underline{\sigma}\, T_{00}$$

$$F_{2m} = \sum_{m'} D^{(2)}_{m'm} F_{2m'} \qquad (7)$$

where $F_{2m'}$ are components of the spherical tensor formed from $\underline{\sigma}$ in the principal axis system and T_{2-m} are components of the spherical tensor in spin coordinates in the laboratory frame. The fluctuations are accounted for by the order parameters, i.e., the average values of Wigner rotation matrix elements:

$$\langle D^{(\ell)}_{m'm} \rangle = \int d\Omega D^{(\ell)}_{m'm}(\Omega)\, P(\Omega) \qquad (8)$$

where $P(\Omega)$ is the probability distribution for orientation of the molecules given by McMillan. I shall not go into the details of these calculations here, since they would take up too much time. They will be published soon.

The results are shown in Fig. 14 as lineshapes at various angles of sample rotation in the magnetic field. The difference between the rotationally frozen (top two) and free rotation (bottom)

cases in the figure is that only in the latter is there a translation of some spectral intensity to the right as the sample is rotated. In Fig. 15 an experimental spectrum of the ortho ^{13}C lines in OAB with the sample rotated at 50° is shown. The spectrum seems to correspond more clearly to the case of free rotation about the long axis and would then appear to rule out the electric dipole model of McMillan, in agreement with the conclusions of Luz and Meiboom in TBBA.

The conclusions of Luz and Meiboom on TBBA have been questioned by Doane et al.[19] based on deuterium spectra in partially deuterated material. However, the model presented by Doane et al. requires a freezing of motion of the benzene rings about their "para" axes. In Fig. 16 I show a ^{13}C spectrum of TBBA taken in the smectic-C phase. Looking at the diagram of the molecule we see that we expect 3 aromatic ortho lines if the benzene rings flip internally rapidly and 6 if they do not. Since only 3 lines are indeed observed, this would appear to confirm unequivocally the internal molecular dynamics in this molecule and to throw doubt again on the conclusion about rotational order in the smectic-C phase of this system.

C. Molecular Motion in Solids[4]

A perennial and difficult question in the study of molecular solids has been that of the mode of molecular motion. In particular, one expects the potential binding rotational motion in the solid state to differ substantially from that in liquid or gaseous environments. Thus, rotational diffusion is usually assumed for fluids whereas transitions between discrete potential minima are more likely in a

0 0 0 0 4 4 0 6 7 5 3

solid. Clearly, it is not simple to investigate experimentally the mode of motion in the solid, since most observable properties are likely to differ very little between the different cases of motion.

To take a particular example, how would one tell what the mode of molecular reorientation is for the solid phases of benzene, a molecule which possesses a six-fold axis of symmetry. It is known that in solid benzene (above 40 K) the molecules are indeed rotating about the six-fold axes at a rate in excess of several kHz, yielding an average of various spectral parameters which fall in this frequency range. But the mode of motion, and the magnitude of the potentials are questions of great interest, in particular for the study of conformational motion and stability of systems of chemical interest.

One set of properties that differentiates between modes of motion are the time-correlation functions:

$$G_{\ell m}(\tau) = \langle T_{\ell m}(0)\ T_{\ell -m}(\tau)\rangle \qquad (9)$$

where $T_{\ell m}$ are components of spherical tensors of rank ℓ, which are related to our normal observables, e.g. dipole moment ($\ell = 1$), quadrupole moment ($\ell = 2$), magnetic shielding tensor ($\ell = 2$), etc., and $\langle\ \rangle$ denotes an ensemble average. Although magnetic resonance is normally a powerful microscopic tool, the $G_{\ell m}(\tau)$ in (9) cannot normally be extracted in full from experiments, and only a small number of points can be provided by relaxation studies. Thus, even though the different modes of motion yield different $G_{\ell m}(\tau)$, it has not been possible to use magnetic resonance to resolve this, and

other approaches such as Raman scattering for direct measurements of (9) are even more difficult.

Baram, Luz, and Alexander (BLA)[20] and Spiess et al.[21] have recently shown that it should be possible to distinguish between modes of motion by direct observation of anisotropic spectral parameters in powdered samples. Some examples have also been reported by these workers. Let us take an example of the magnetic shielding tensor $\underset{\sim}{\sigma}$ for the aromatic nuclei in hexamethylbenzene. This has a six-fold axis like benzene but it is easier to handle experimentally. Using expansion techniques, developed in collaboration with Freed at Cornell University, BLA have calculated the lineshapes for two extreme modes of motion: (a) the molecule jumps between discrete sites corresponding to the minima in a six-fold potential, (b) random jumps between all sites about the six-fold axis. In the region where the rate of rotations is of the order of the magnetic shielding anisotropy, they predict a striking difference in powder lineshapes. No experiments were done on this particular system.

We show here some direct calculations which we have done on the above system, together with experimental results. Our calculations are "exact" in the sense that they represent a direct computer solution of the secular equations of motion, and they do indeed bear out the elegant asymptotic calculations of BLA.

Figure 16 indicates the basis of the problem. The powder sample consists of molecules at all orientations in space, namely an isotropic distribution in angles (β,γ) in the figure. These molecules reorient

0 0 0 0 4 4 0 6 7 5 4

about their six-fold axes. Let us denote as before by σ the observed parameter of the tensor $\mathcal{Q}$, i.e., the chemical shift, and by $I_m(\sigma)$ the spectrum of a molecule with orientation Ω in space. Then the observed powder spectrum $I(\sigma)$ is given by:

$$I(\sigma) = \int I_m(\sigma)\ P(\Omega)\ d\Omega \tag{10}$$

where $P(\Omega)$ is the orientational probability distribution function and $I_m(\sigma)$ is clearly a function of Ω. To calculate $I_m(\Omega)$ we assume that the molecule reorients by discrete jumps between sites in a symmetrical n-fold potential. It can then be shown that $I_m(\sigma)$ is given by:

$$I_m(\sigma)\ \alpha\ \ \mathrm{Re} \sum_{j=1}^{n} \sum_{k=1}^{n} A_{jk}^{-1} \tag{11}$$

A_{jk}^{-1} are the elements of a matrix $\underset{\approx}{A}^{-1}$ which is the inverse of a relaxation matrix $\underset{\approx}{A}$, with

$$A_{jk} = -\tau_{jk}^{-1}, \quad j \neq k$$

$$A_{jj} = i(\sigma-\sigma_j) + \sum_{k\neq j} \tau_{jk}^{-1} + T_2^{-1} \tag{12}$$

The parameters which appear in this matrix are:

τ_{jk}^{-1}: probability of a transition from site j to k

σ_j : the observed shift for site j

T_2^{-1}: natural homogeneous linewidth for σ.

The only missing ingredient then is the dependence of σ on Ω which is straight forward since $\underset{\sim}{\sigma}$ transforms as a second rank tensor. Since we work in high magnetic field, the observable $\underset{\sim}{\sigma}$ is the zero order component of the spherical tensor which goes with T_{20}, i.e., σ_{zz} in the laboratory frame.

We have solved the lineshape Eq. (11) for the two cases n = 6 and n = 24. The first corresponds to the case of a discrete six-fold potential whereas the latter already approximates well the lineshapes for the case of continuous rotational diffusion. As shown by group theoretical arguments,[20] only one parameter is required to describe the motion for six-fold jumps, (D_6) since the observable is related to a second rank tensor and belongs to D_2. The only relevant representation induced in D_6 by the totally symmetric irreducible representation of D_2 is E_2.[20] Thus, τ^{-1} is used as the single parameter to correlate with the experimental dependence of lineshape on temperature.

Figure 17 shows theoretical spectra calculated in this way for various values of τ in the two cases. The case n = 24 is on the left. Only the left edge of the powder calculations are shown. Values for σ_{11}, σ_{22} and σ_{33} were taken from measurements at low temperature, and the angles Ω in (10) were determined by assuming that the symmetry of $\underset{\sim}{\sigma}$ is the same as the local molecular symmetry at the nucleus. Note the smooth transition from spectra in the low temperature (low τ^{-1}) regime where the molecules are rigid to the high temperature (high τ^{-1}) case where they rotate rapidly about their six-fold axes.

0 0 0 0 4 4 0 6 7 5 5

In contrast to this, the right side of Figure 17 shows the calculated spectra for the case n = 6. Here, instead of a smooth, featureless transition, structure is seen which is quite characteristic of the symmetry of the potential. The experimental results for polycrystalline hexamethylbenzene are shown in Figure 18, and we see that they conform more closely to the case of six-fold discrete jumps in Figure 17, in particular the spectra at -135.8°C and -130.6°C. The full experimental spectrum at -135.8°C appears in Figure 19(a) and Figure 19(b) shows a comparison of part of the spectrum at -135.8°C with the appropriate theoretical spectrum calculated for the six-fold jumps.

Thus, this technique appears to provide a sensitive way of determining details of molecular motion. We are currently in the process of calculating the magnitude of the hindering potential from these results and are also extending the work to other molecular solids and potential symmetries.

I note here that discussions with Professor Luz and Dr. Baram were extremely helpful in understanding some problems related to this work.

D. Proton Chemical Shielding Tensors

The water sample used was enriched to greater than 99% in deuterium and the residual protons observed. The deuterium spins were decoupled as described previously. Figure 20 shows proton spectra in ice at -90°C with and without deuterium decoupling, showing in the latter a resolution of the ^{1}H chemical shielding

anisotropy. The values of the principal elements are, relative to TMS:[8]

$$\sigma_{\parallel} = 15 \pm 2 \text{ ppm}$$

$$\sigma_{\perp} = -19 \pm 2 \text{ ppm}$$

Yielding an anisotropy of $\Delta\sigma = 34 \pm 4$ ppm which is similar to those measured for some hydrogen-bonded protons in organic acids.[22] We have measured other new tensors in this way and results will be presented elsewhere.

E. Proton Dynamics in Ice

Figure 21 shows spectra of the residual protons in heavy water at several temperatures. It is clear that some sort of motional process of the protons is taking place, averaging the shielding tensors to its isotropic value. This is not surprising and is in agreement with what is known from previous wideline nmr studies.[23] However, here we see for the first time the direct effect of motion on the high resolution spectra--as we've seen earlier, this should give us a sensitive way of determining the type of motion taking place.

Indeed, we notice that the transition from low to high temperature spectra is not smooth, and a weak singularity is appearing near the isotropic position (for example, observe the spectra at -60°C and -52.5°C). These are exactly the features expected for motion in a potential with cubic type symmetry[20,21] e.g., tetrahedral. Now, as shown in Figure 22, the oxygen environment in ice I has near

0 0 0 0 4 4 0 6 7 5 6

tetrahedral symmetry, so there are 6 almost equivalent positions of the water molecule, corresponding to the low energy Slater configurations with two protons in hydrogen bonds close to the oxygen. Transitions between these configurations take place by motion of defects, e.g., Bjerrun faults[23] as shown in Figure 23, or vacancy diffusion. The latter is currently favored.[23]

From the spectra alone, we cannot distinguish between the mechanisms, but we clearly can separate the reorientational motion from translational motion, a clear advantage over spin relaxation measurements. We are currently extracting quantitative information from our measurements.

I think that this gives you some idea of the potential of these techniques, so I shall stop here and leave other details to the scientific literature and to our future meetings.

ACKNOWLEDGMENTS

Various aspects of this work were supported by the National Science Foundation, Research Corporation, NATO, and the Materials and Molecular Research Division of the Lawrence Berkeley Laboratory. Dr. Höhener had a postdoctoral fellowship of the Petroleum Research Fund administered by the American Chemical Society. I am grateful for extremely helpful discussions with Professors Michael Mehring, Robert Blinc, Zeev Luz, Erwin Hahn, and Jim Emsley. I also thank Dr. Ulrich Haeberlen and Professor Michael Mehring for permitting me to see preprints of their review articles (ref. 22).

Table I. $^{13}COO^-$ Shielding Tensors

Compound	σ_{11}	σ_{22}	σ_{33}	$<(\sigma_{33},\perp)^a$	$<(\sigma_{\parallel},C\text{-}C)^b$
alanine	-116 ± 2	-56 ± 2	19 ± 2	3 ± 4	10 ± 4
malonic acid	-114 ± 2	-48 ± 2	23 ± 4	0 ± 2[c]	32 ± 2
ammonium hydrogen malonate	-113 ± 2	-46 ± 3	26 ± 2	3 ± 3	25 ± 3
ammonium tartrate	-111 ± 3	-62 ± 4	22 ± 2	7 ± 3	4 ± 3

[a] angle between σ_{33} and perpendicular to $^{13}COO^-$ plane

[b] angle between σ_{11} and C-C direction bisecting CO bonds

[c] imposed on tensor, not by X-ray orientation

0 0 0 0 4 4 0 6 7 5 7

References

1. M. Mehring, G. Sinning, A. Pines and T. W. Shattuck, paper presented at this meeting.
2. A. Pines, M. G. Gibby and J. S. Waugh, J. Chem. Phys., 59, 569 (1973), Chem. Phys. Lett., 15, 373 (1972).
3. R. K. Hester, J. L. Ackerman, V. R. Cross and J. S. Waugh, Phys. Rev. Lett., 34, 993 (1975).
4. D. J. Ruben, D. E. Wemmer, and A. Pines, to be published; A. Pines, Lawrence Berkeley Report no. 3530, Inorganic Materials Research Division Annual Review, 1975.
5. U. Haeberlen and J. S. Waugh, Phys. Rev., 175, 453 (1968).
6. R. C. Hewitt, S. Meiboom and L. C. Snyder, J. Chem. Phys., 58, 5089 (1973); L. C. Snyder and S. Meiboom, J. Chem. Phys., 58, 5096 (1973).
7. J. W. Emsley and J. W. Lindon, NMR in Liquid Crystals, Pergamon, in press, 1975.
8. A. Pines, D. J. Ruben, S. Vega and M. Mehring, to be published.
9. J. J. Chang, R. G. Griffin and A. Pines, J. Chem. Phys., 60, 2561 (1974); J. Kempf, H. W. Spiess, U. Haeberlen and H. Zimmerman, Chem. Phys., 4, 269 (1974).
10. A. Pines, J. J. Chang and R. G. Griffin, J. Chem. Phys., 61, 1021 (1974); A. Pines and J. J. Chang, Proceedings of the 18th Ampere Congress, Nottingham, England, September, 1974.
11. D. J. Ruben, in preparation; to be submitted as a Lawrence Berkeley Laboratory report.

12. A. Pines, D. J. Ruben and S. Allison, Phys. Rev. Lett., 33, 1002 (1974); A. Pines and J. J. Chang, Phys. Rev. A., 10, 946 (1974).

13. S. Pausak, A. Pines and J. S. Waugh, J. Chem. Phys., 59, 591 (1973).

14. J. J. Chang, R. G. Griffin and A. Pines, J. Chem. Phys., 62, 4923 (1975).

15. Z. Luz and S. Meiboom, J. Chem. Phys. 59, 275 (1973); Z. Luz, R. C. Hewitt and S. Meiboom, J. Chem. Phys., 61, 1758 (1974).

16. R. A. Wise, D. H. Smith and J. W. Doane, Phys. Rev. A, 7, 1366 (1973).

17. W. L. McMillan, Phys. Rev. A., 8, 1921 (1973).

18. S. A. Allison, M. S. Thesis, Berkeley, 1975, unpublished.

19. J. W. Doane, private communication of details from talk presented at the International Liquid Crystals Conference, Stockholm, Sweden, June, 1974.

20. A. Baram, Z. Luz, and S. Alexander, J. Chem. Phys., in press. See also S. Alexander, A. Baram and Z. Luz, Mol. Phys., 27, 441 (1974).

21. H. W. Spiess, Chem. Phys., 6, 217 (1974); H. W. Spiess, R. Grosesin and U. Haeberlen, Chem. Phys., 6, 226 (1974).

22. (a) U. Haeberlen in Advances in Magnetic Resonances, Academic, New York, in press.

(b) M. Mehring in NMR, Basic Principles and Progress, Springer-Verlag, Berlin, in press.

23. For example, D. E. Barnaal and I. J. Lowe, J. Chem. Phys., 48, 4614 (1968), J. Chem. Phys., 46, 4800 (1967); L. Onsager and L. K. Runnels, J. Chem. Phys., 50, 1089 (1969); R. Blinc, G. Lahajnar and I. Zupancic, Chem. Phys. Lett., 4, 363 (1969).

0 0 0 0 4 4 0 6 7 5 8

Figure Captions

1. Normal spin-decoupled free induction decay for high resolution nmr of rare nuclear spins.
2. Orientation of principal axes of the ^{13}C shielding tensor for an isolated $^{13}COO^-$ group.
3. Hydrogen-bonding in solid carboxylic acids.
4. Spectral distribution for dipolar-coupled (D) proton deuterium pair. The deuterium quadrupole is characterized by an axial field gradient giving an external splitting Q >> D. Shown are typical oriented pair (middle) and powder (bottom) spectra. The deuterium resonance in the powder is spread over a large range of frequencies (Q $\sim$ 100 kHz) which would appear to make deuterium decoupling impossible in the solid.
5. (a) Transitions for deuterium spin with applied field ω_1. The allowed transitions ω_A and ω_B occur with probability $P \sim \omega_1^2$ at resonance and the two-quantum transition at ω_0 occurs with $P \sim \omega_1^4/Q^2$ at resonance. (b) Summary of simple deuterium decoupling conditions from back-of-envelope calculation.
6. Application of deuterium decoupling to perdeuterated dimethylsulfoxide (DMSO). Shown are the Fourier transforms of the decays of the residual protons in solid DMSO-d_6 undecoupled, solid DMSO-d_6 deuterium decoupled, and isotropic.
7. Dependence of proton linewidth on deuterium decoupling offset frequency (measured from the center of the deuterium line, i.e., isotropic position). The extreme sensitivity to frequency for low ω_1 of the deuterium is characteristic for the double-quantum process.

8. Schematic diagram of radio frequency part of spectrometer for ^{13}C-^{1}H and ^{2}H-^{1}H double-resonance experiments.

9. Schematic diagram of double-resonance probe for solid and liquid crystal work.

10. MBBA molecule and orientation of principal axes of ^{13}C shielding tensors for two prime functional groups, aromatic and aliphatic.

11. Change of proton decoupled ^{13}C spectra of MBBA in isotropic-nematic transition. These spectra have been used to extract information on molecular ordering, end chain effects, conformational motion, etc., in a number of nematic and smectic liquid crystals.

12. Schematic diagram of domain structure and effect of magnetic field rotation in smectic-C phase.

13. Tilting of molecules in smectic-C phase due to transverse electric dipoles, after McMillan.

14. Calculated lines for "ortho" aromatic ^{13}C nucleus showing effect of sample rotation in a magnetic field for a smectic-C phase with tilt angle of 45° and 10° between para axes and long molecular axis (planar molecules). The model for domain behavior used is that of Luz et al. (reference 15). For each model calculated lineshapes are shown for sample orientation of 0 through 90°. Top figure: full nematic order (S = 1) and full rotational order about long axis, with 180° flips of benzene rings, minimum diamagnetic susceptibility along long molecular axis. Middle figure: same, but minimum diamagnetic susceptibility perpendicular to long molecular axis. Bottom figure: full nematic order, but free rotation of molecules about long molecular axes; other parameters the same. Note that only here is there a shift of spectral intensity up field as the sample is rotated.

0 0 0 0 4 4 0 6 7 5 9

15. ^{13}C nmr shape observed for the two 'ortho' lines in smectic-C p-octyloxyazoxybenzene, the 8-carbon chain analog of PAA. The sample has been rotated 55° in the magnetic field, and the isotropic line positions (i.e., at 0° rotation) are shown by vertical bars. Note the shift of spectral density upfield (to the right) corresponding to the model of free molecular rotation.
16. Orientation of rotating molecules in powder sample.
17. Calculated powder spectra for benzene jumps. Left Side: in a 24-fold potential approximating random jump strong collision model. Right side: Same for a six-fold potential. Here the use of one transition parameter is rigorous as explained in the text. Note the peculiar weak sideband features in this case. The numbers next to the spectra are the transition rates between sites in Hz.
18. Left side of experimental spectra for aromatic ^{13}C nuclei in polycrystalline hexamethylbenzene.
19. (a) Full experimental ^{13}C spectrum of hexamethylbenzene at -135.8°C. The arrows depict the expected position of the singularities.
    (b) Comparison of experimental (-135.8°C) and theoretical (τ^{-1} = 400 Hz) spectral regions for six-fold jumps.
20. Spectra of residual protons in heavy (per deuterated) ice -I at -90°C. Deuterium decoupling reveals the chemical shielding anisotropy. Other details appear in the text.
21. Dependence of deuterium decoupled ^{1}H spectra in heavy ice on temperature. The lineshapes can be understood on the basis of proton motion in a potential with tetrahedral symmetry.

22. Six positions of water molecule (i.e., of low energy Slater configurations for protons in hydrogen bonds) in ice.

23. One possible mechanism for reorientation (pseudorotation) of water molecules in ice, the migration of a Bjerrum fault.

0 0 0 0 4 4 0 6 7 6 0

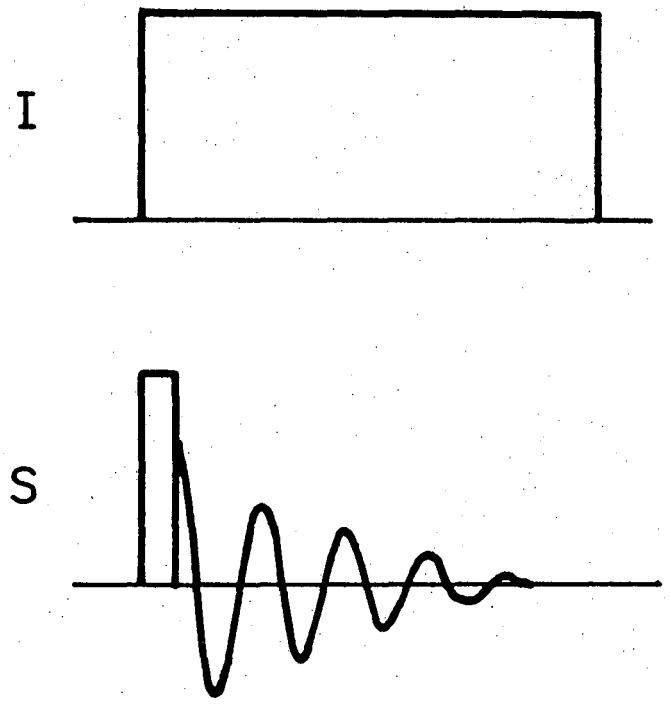

XBL758-6988

Figure 1

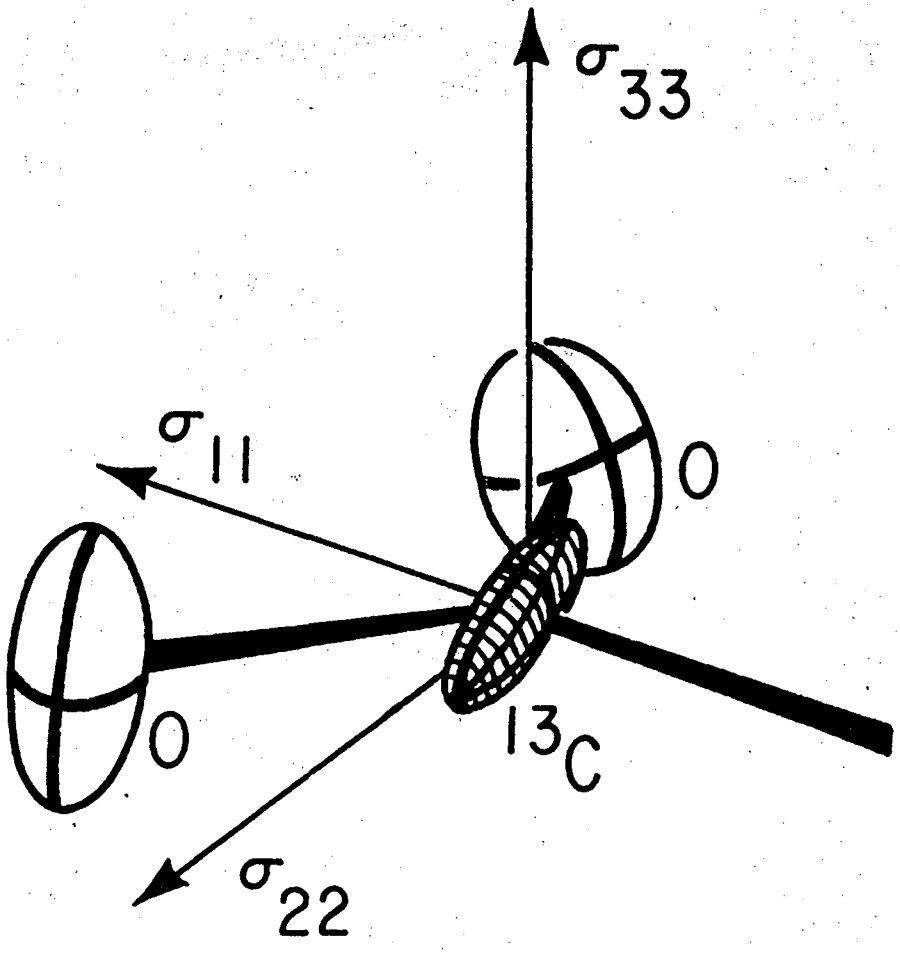

XBL 742-5591

Figure 2

0 0 0 0 4 4 0 6 7 6 1

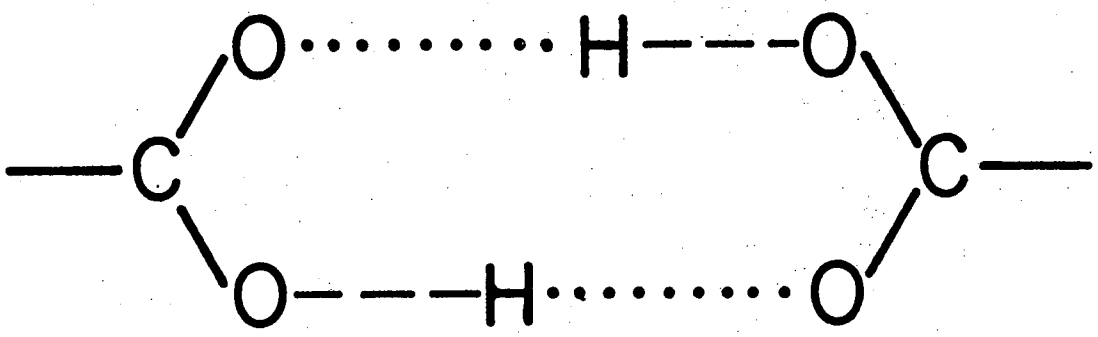

XBL 751-5549

Figure 3

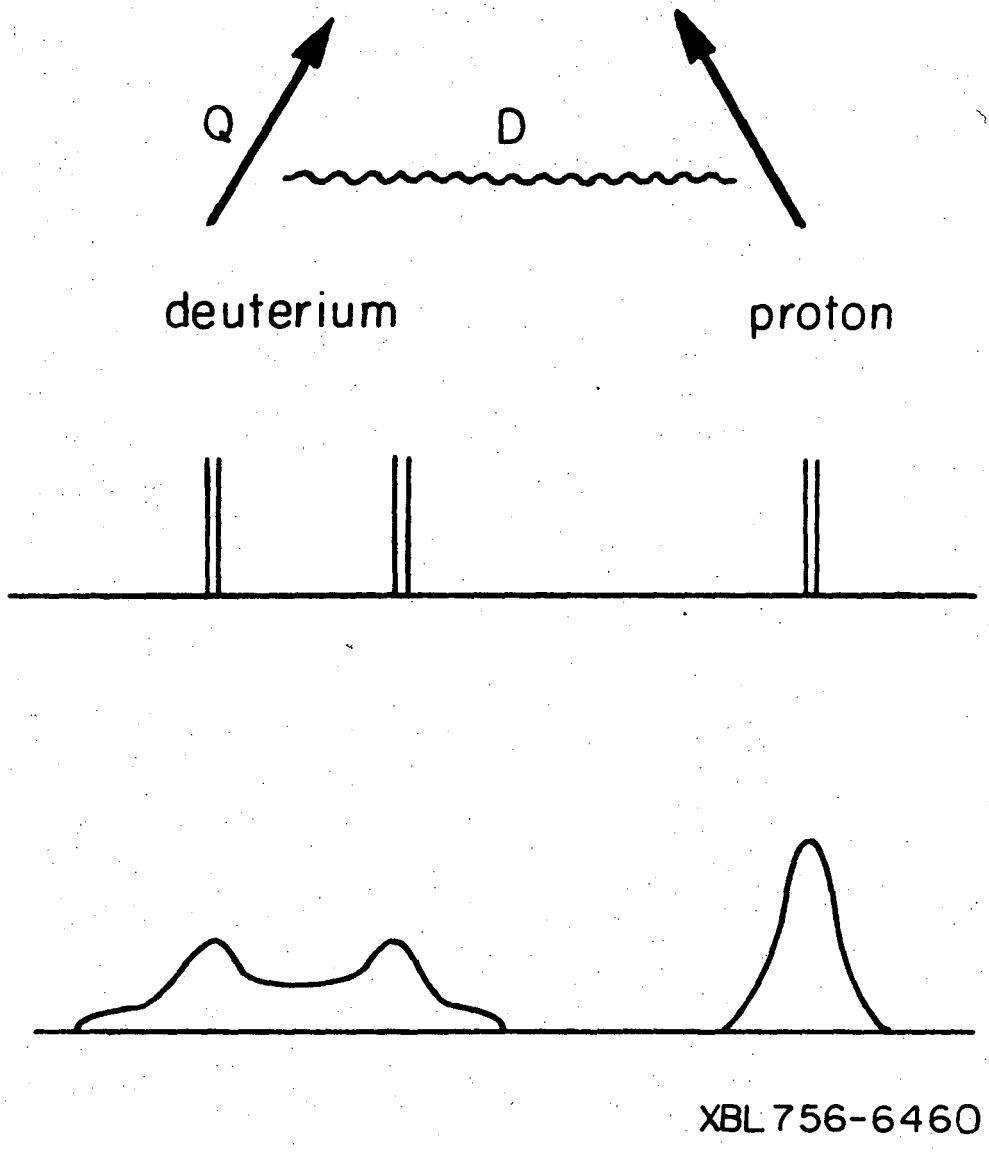

Figure 4

0 0 0 0 4 4 0 6 7 6 2

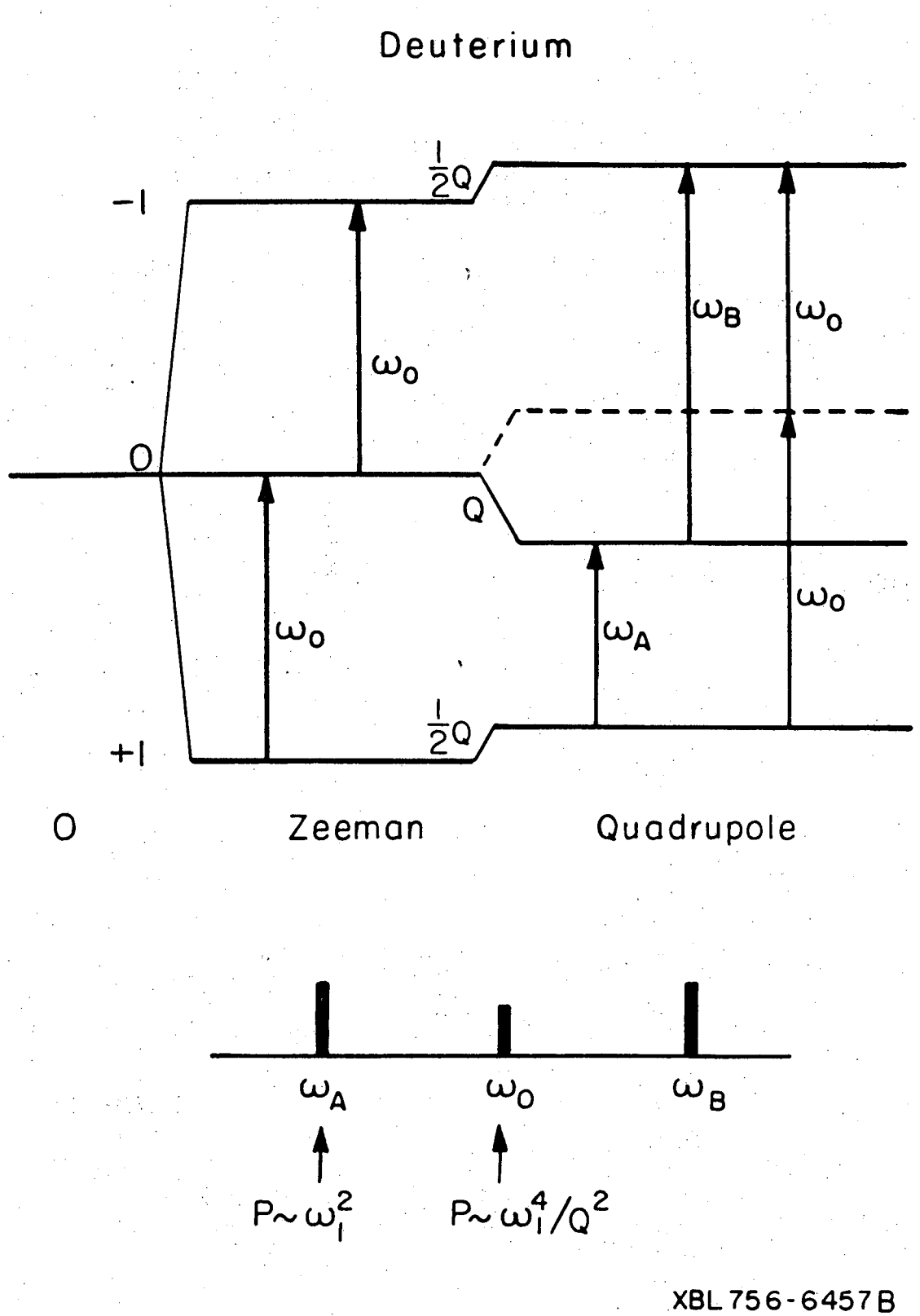

Figure 5(a)

Deuterium Decoupling
($Q \gg D$)

Single Quantum, on resonance

$$\omega_1^2 \sim D^2$$

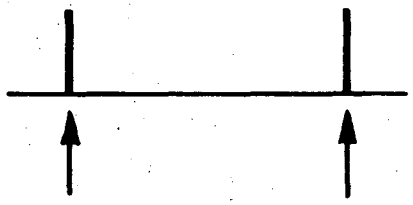

Single Quantum, off resonance by Q

$$\omega_1^2 \sim Q^2$$

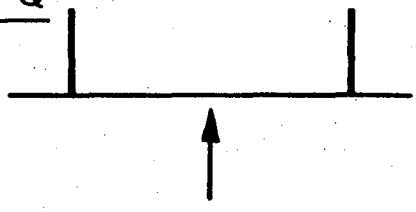

Double Quantum, on resonance

$$\omega_1^2 \sim DQ$$

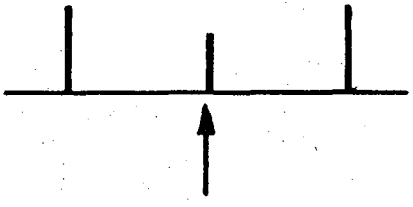

XBL756-6458

Figure 5(b)

0 0 0 0 4 4 0 6 7 6 3

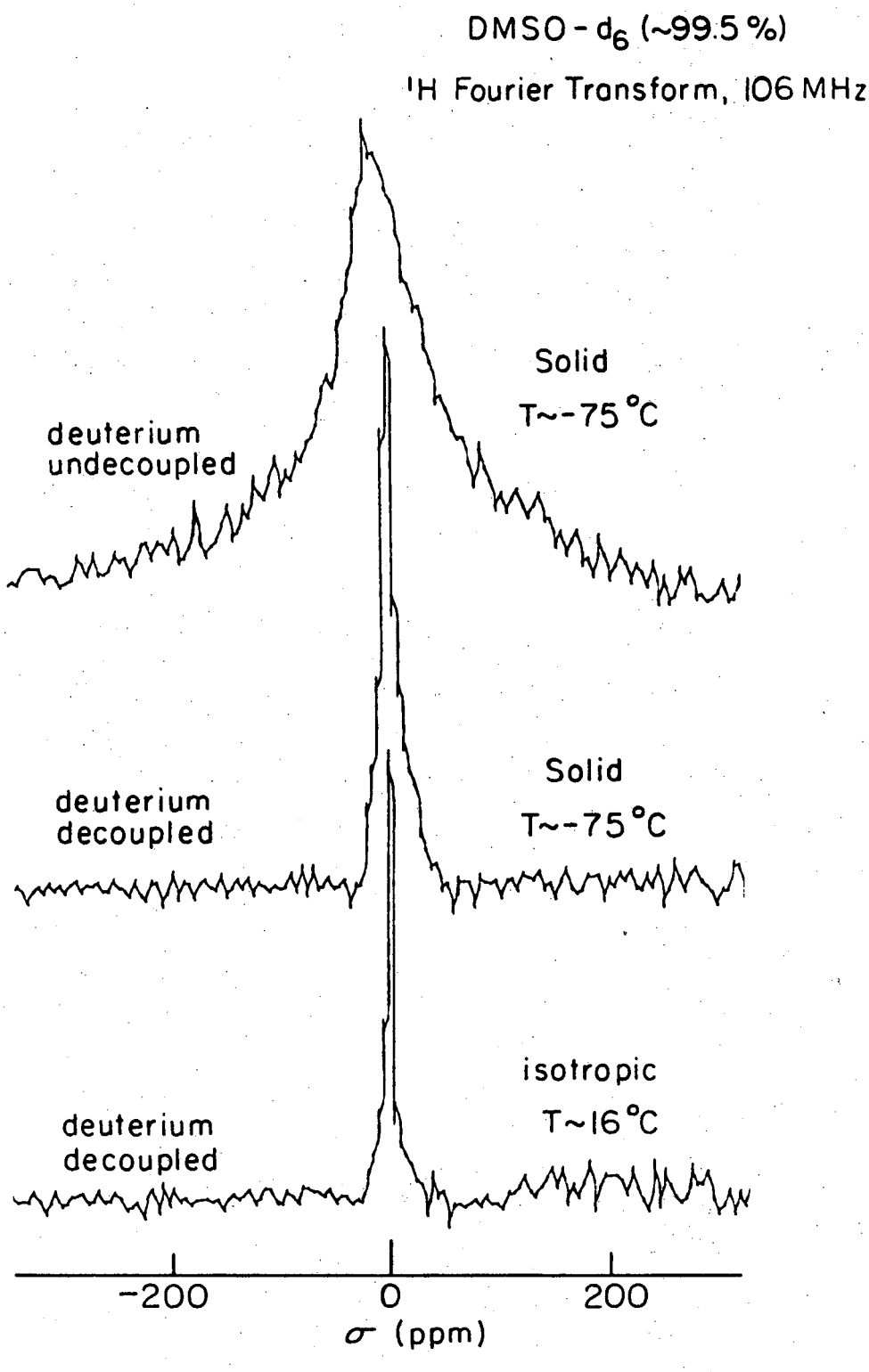

Figure 6

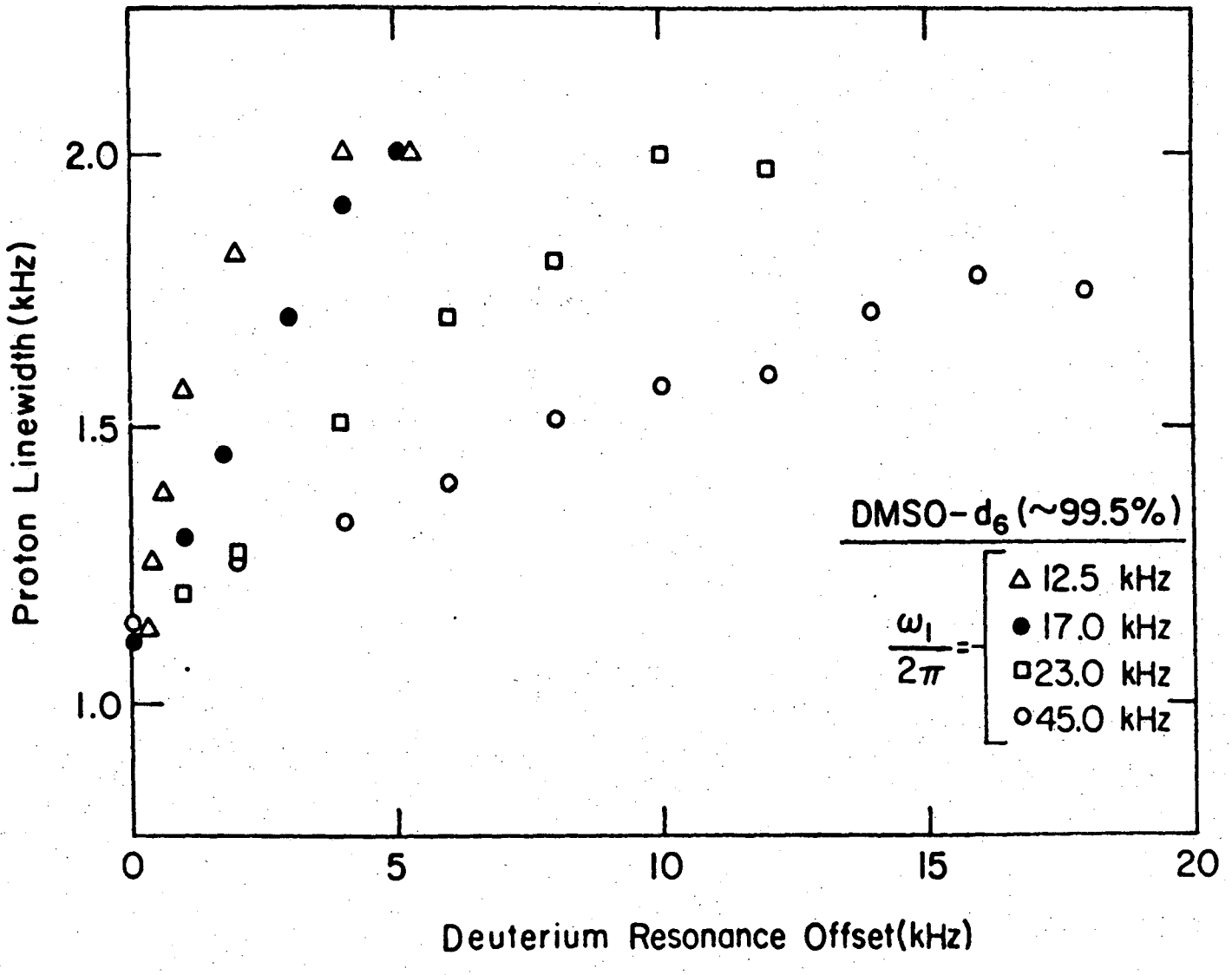

XBL 759-8286

Figure 7

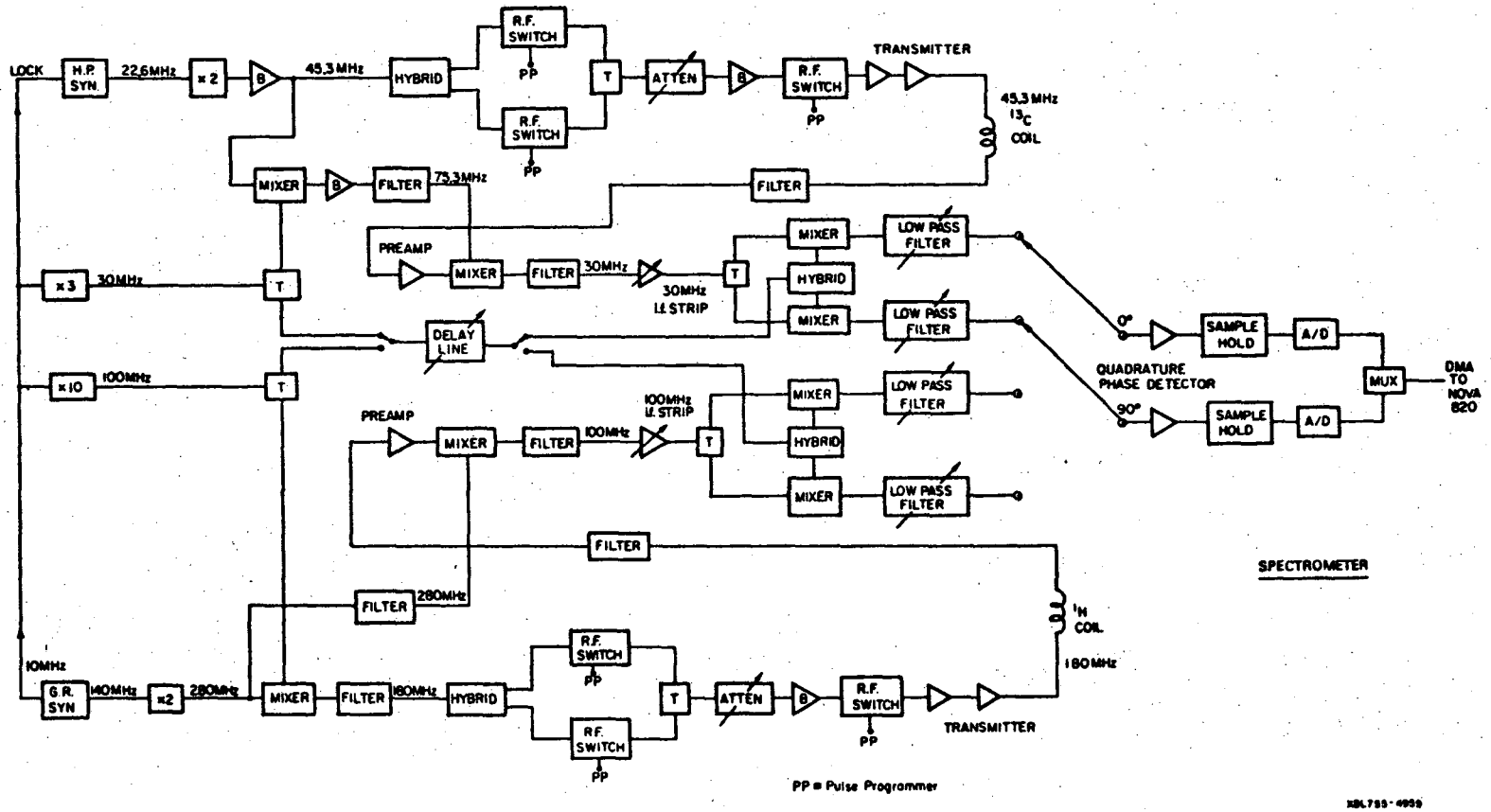

Figure 8

0006764

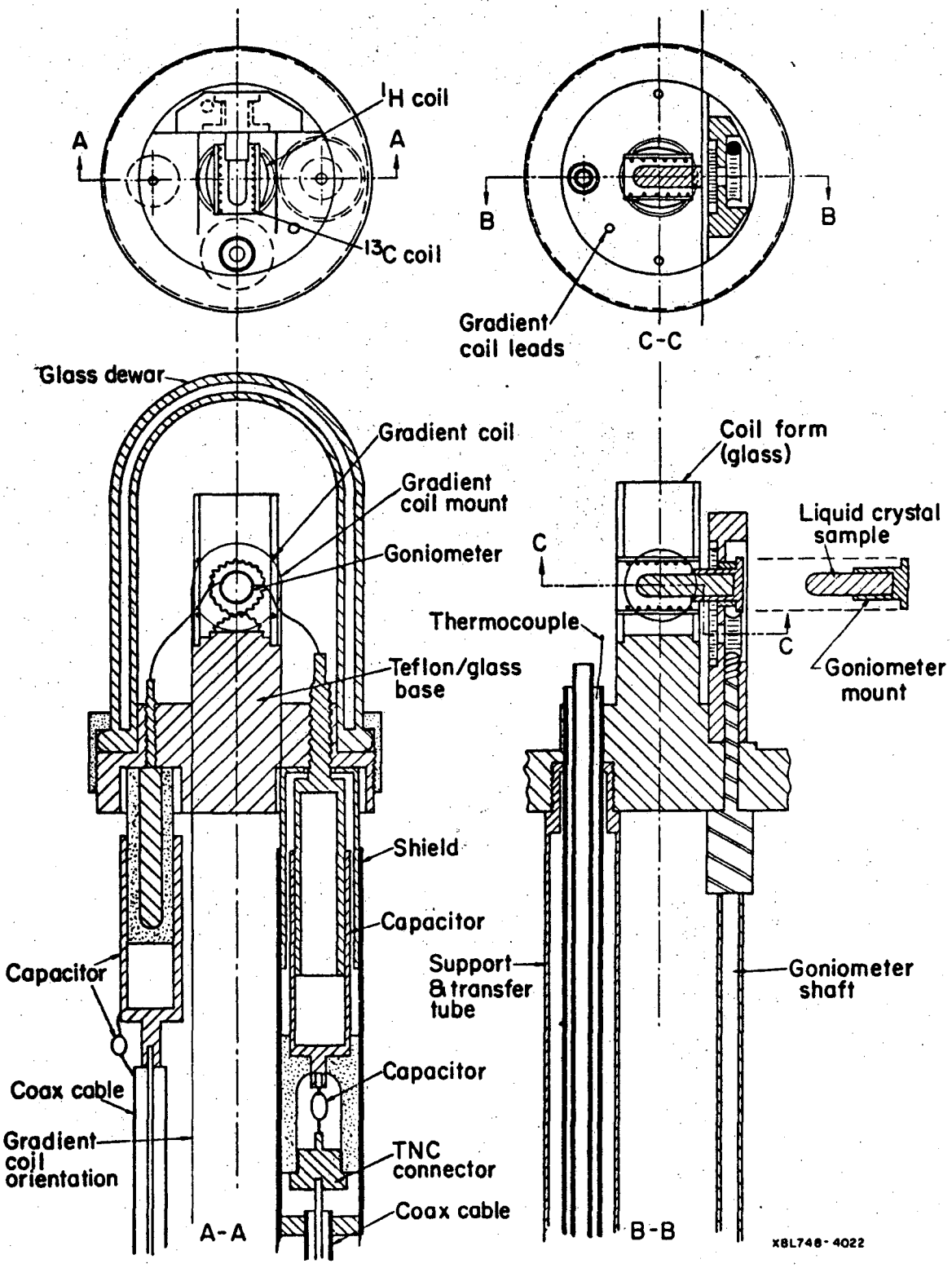
^{1}H coil
^{13}C coil
A
A
B
B
Gradient coil leads
C-C
Glass dewar
Gradient coil
Gradient coil mount
Goniometer
Teflon/glass base
Shield
Capacitor
Capacitor
Coax cable
Gradient coil orientation
Capacitor
TNC connector
Coax cable
A-A
Coil form (glass)
Liquid crystal sample
C
C
Thermocouple
Goniometer mount
Support & transfer tube
Goniometer shaft
B-B
XBL748-4022

Figure 9

0 0 0 0 4 4 0 6 7 6 5

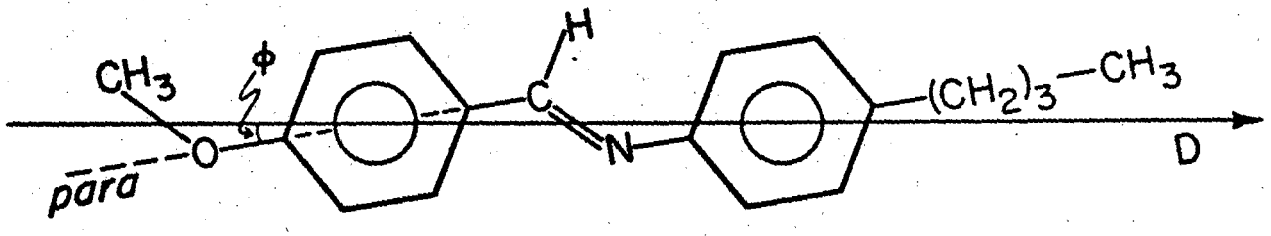

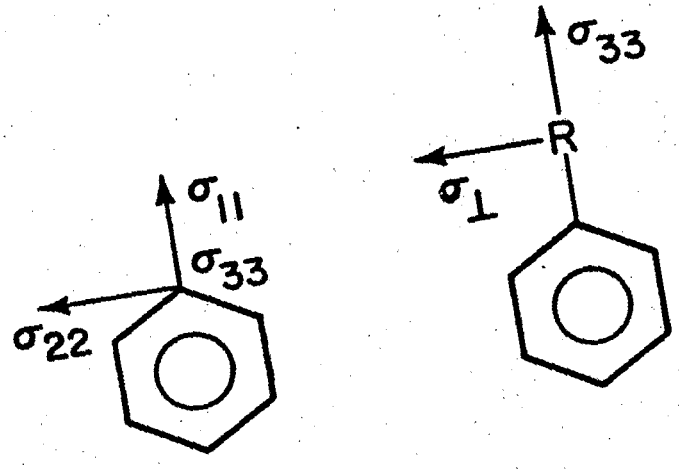

XBL 752-5832a

Figure 10

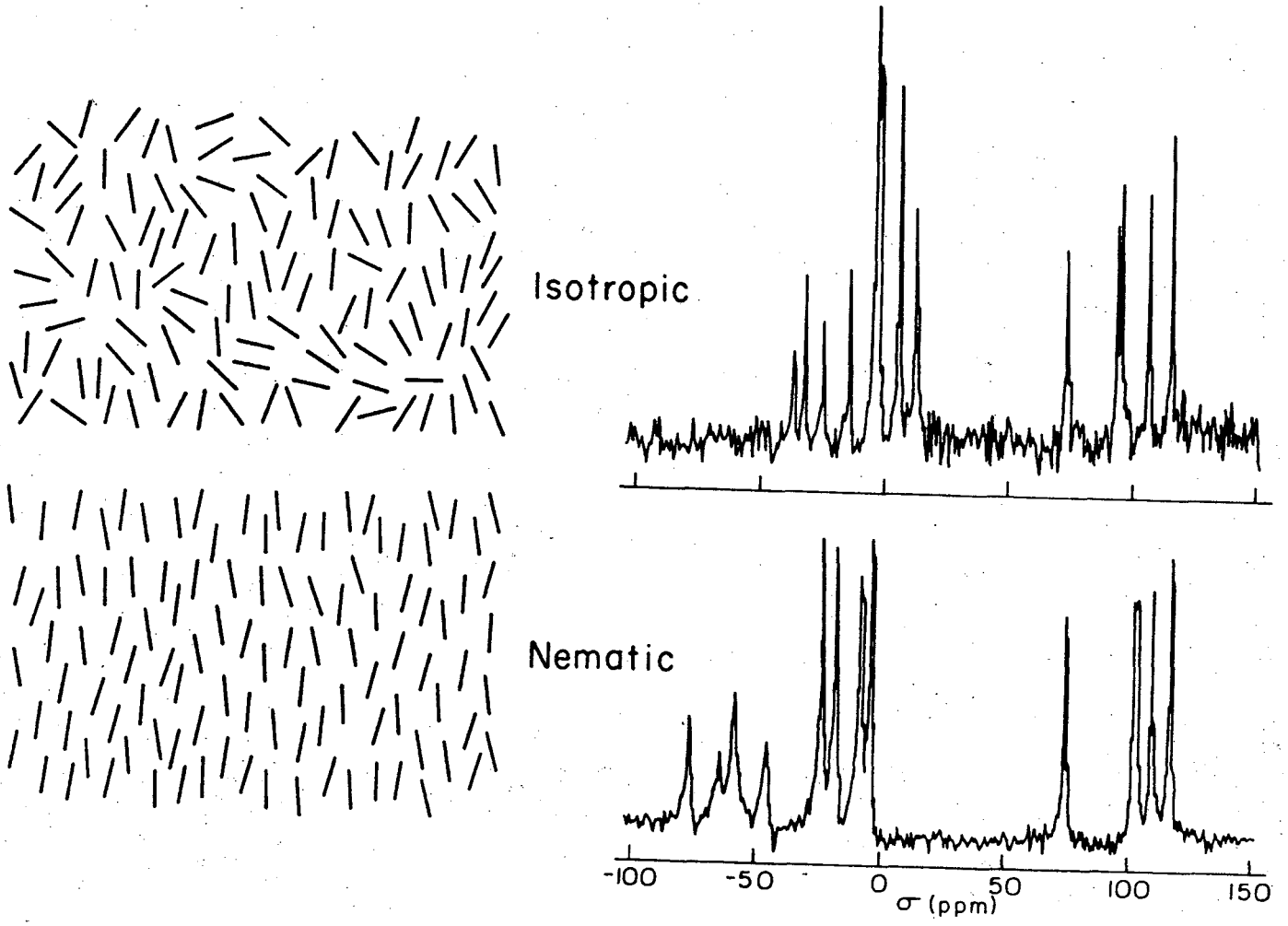

XBL 751-5492

Figure 11

0 0 0 0 4 4 0 6 7 6 6

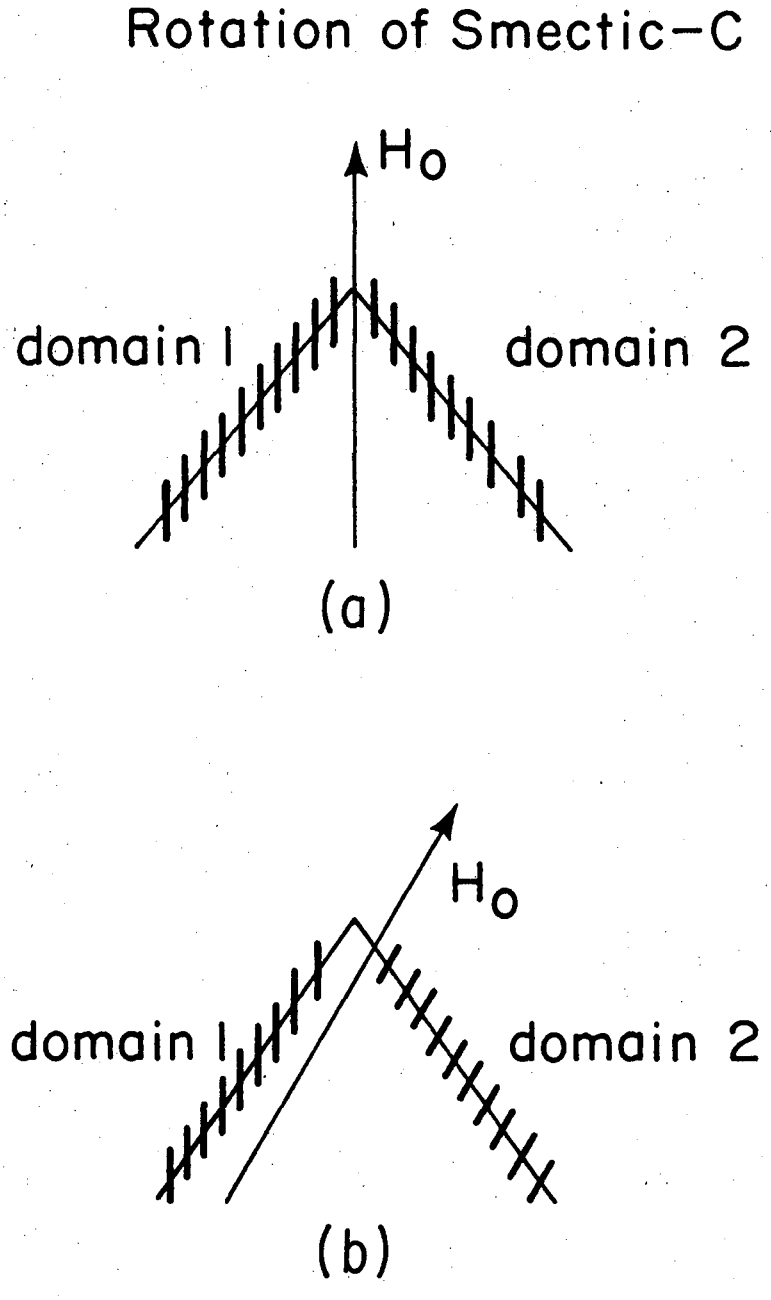

XBL 751-5494

Figure 12

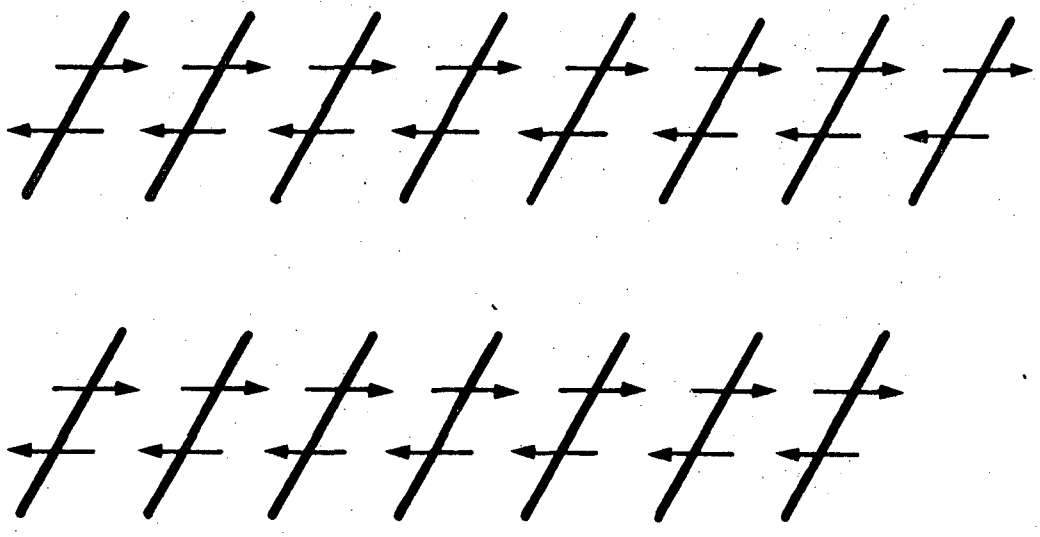

XBL 751-5436

Figure 13

0 0 0 0 4 4 0 6 7 6 7

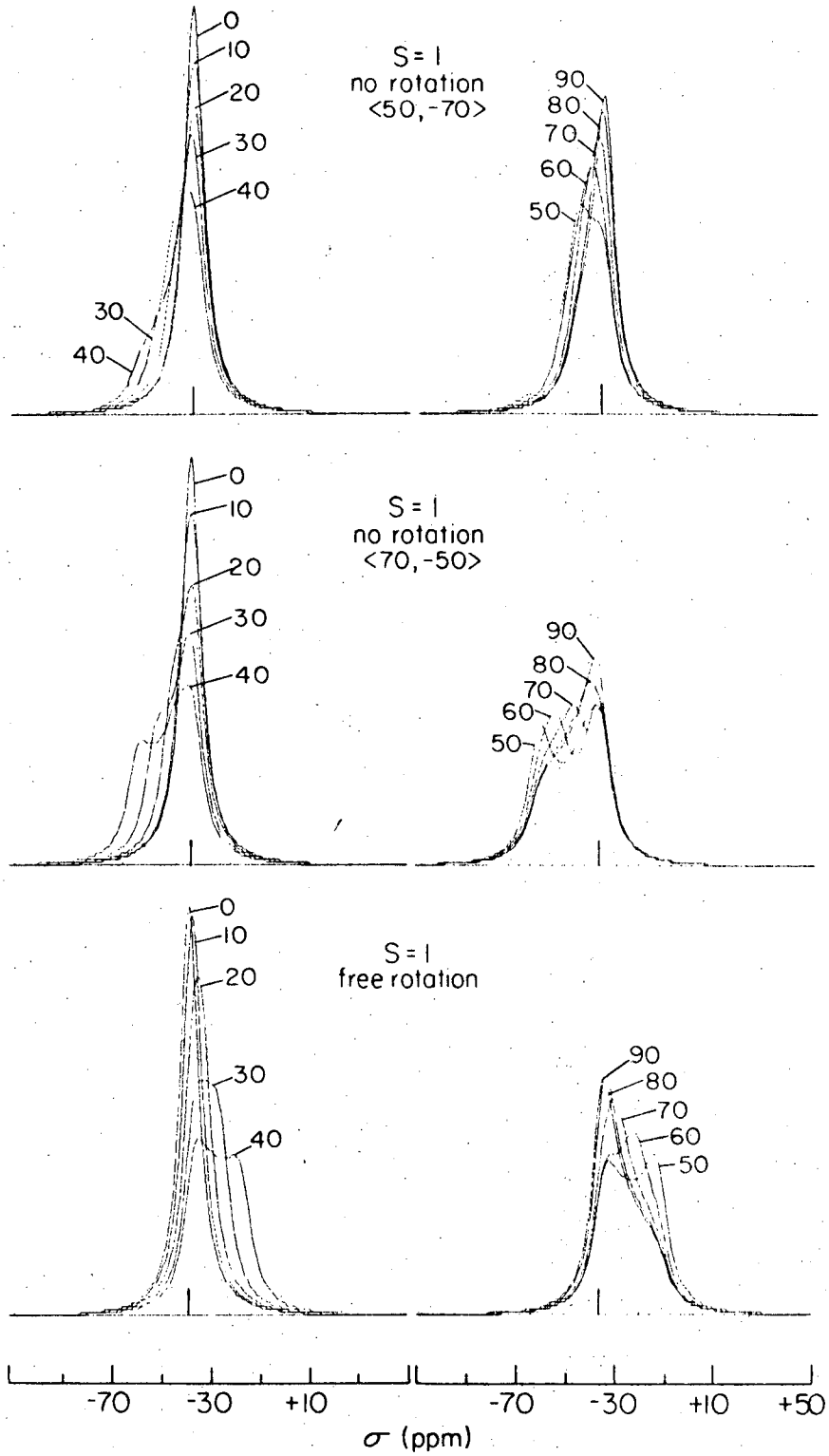

XBL 756-6472

Figure 14

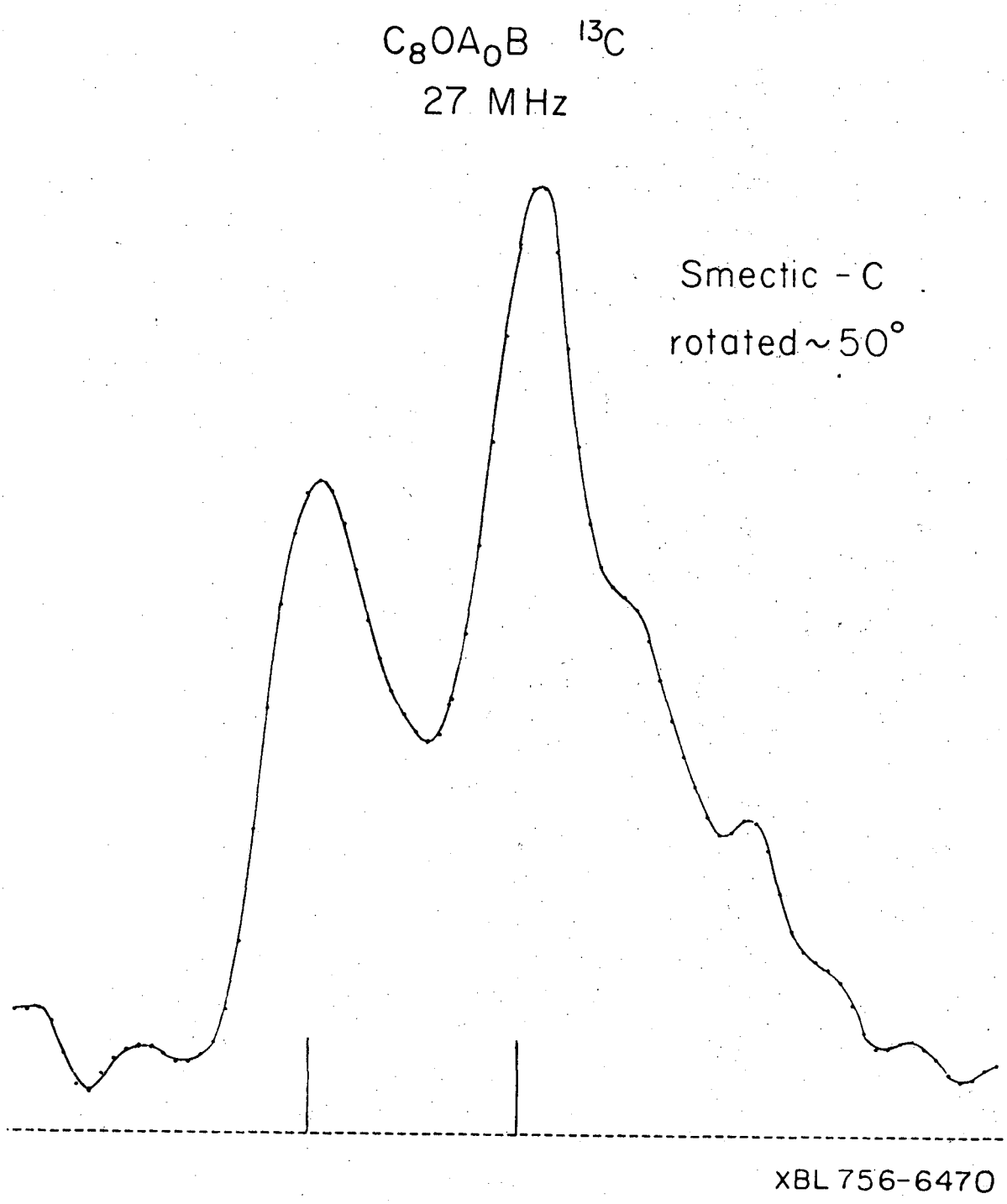

Figure 15

0 0 0 0 4 4 0 6 7 6 8

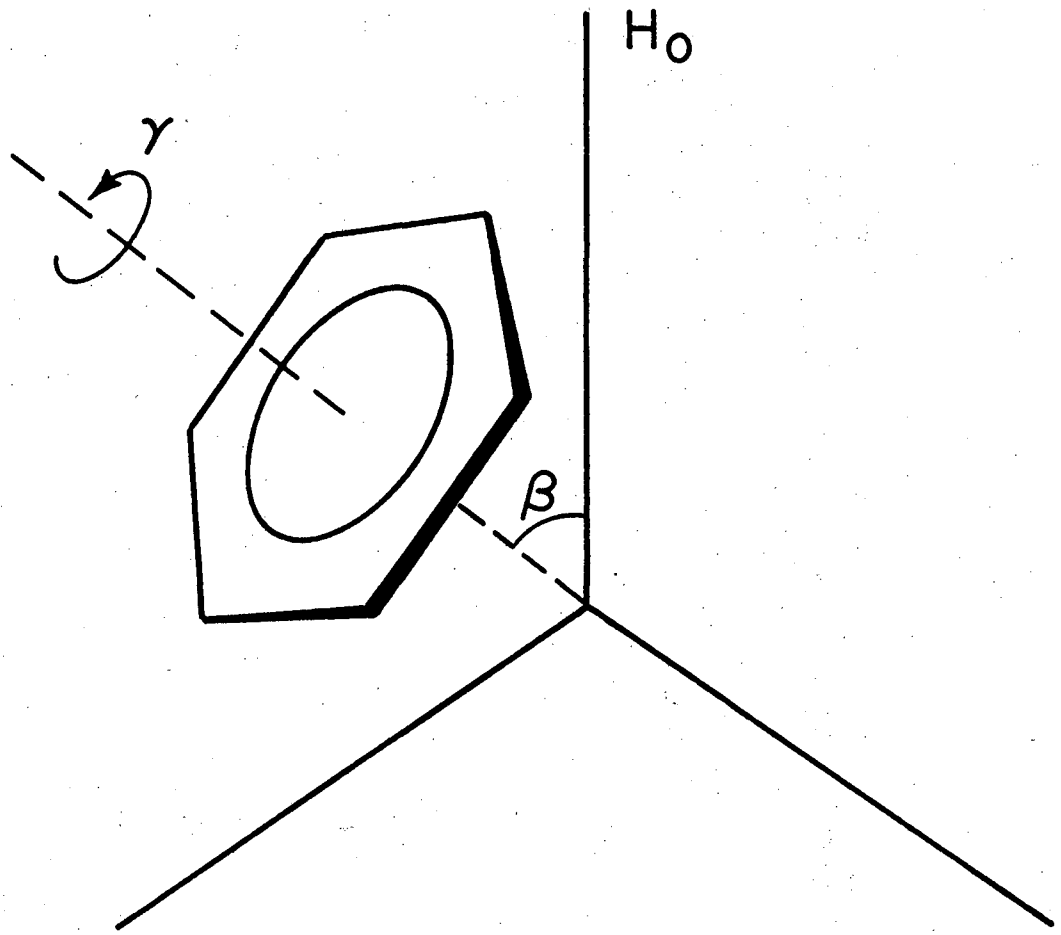

XBL 751-5546

Figure 16

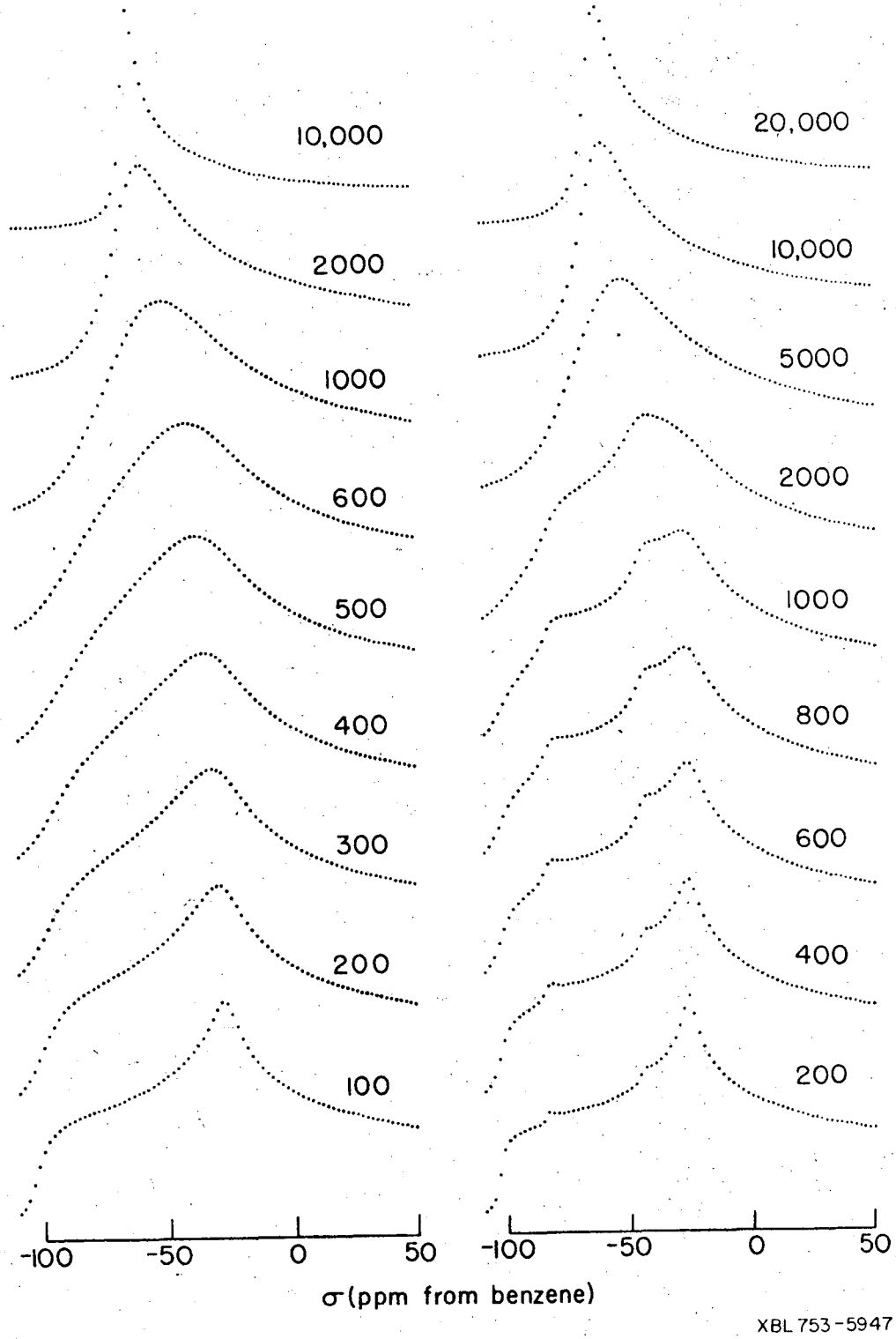
10,000
2000
1000
600
500
400
300
200
100
20,000
10,000
5000
2000
1000
800
600
400
200
-100
-50
0
50
-100
-50
0
50
σ (ppm from benzene)
XBL 753-5947

Figure 17

0 0 0 0 4 4 0 6 7 6 9

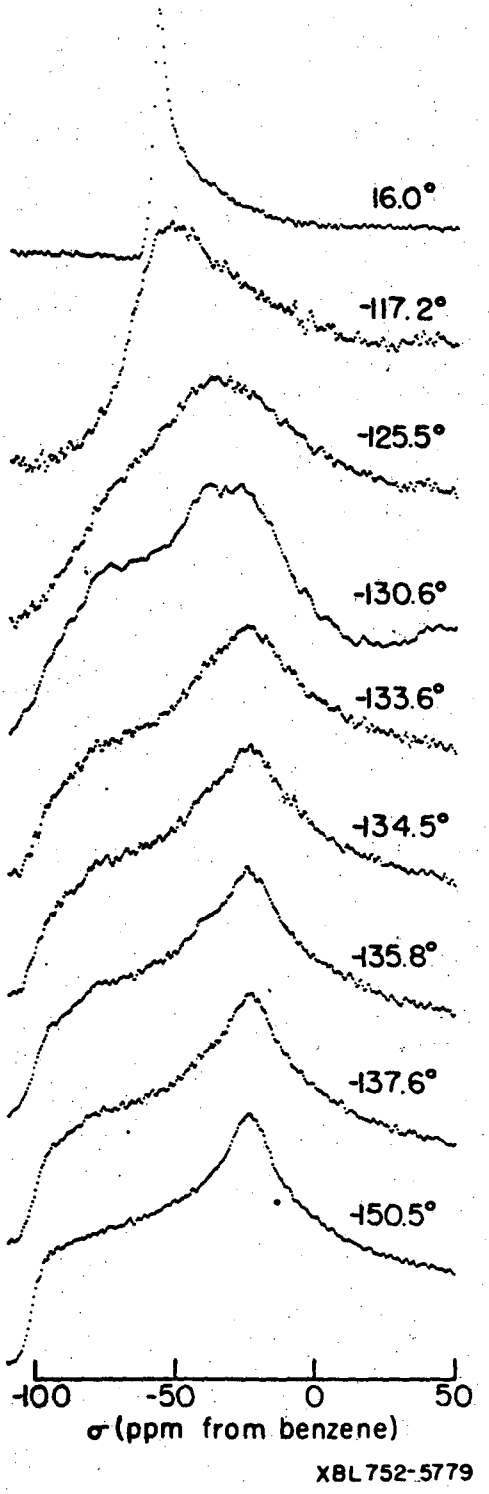

Figure 18

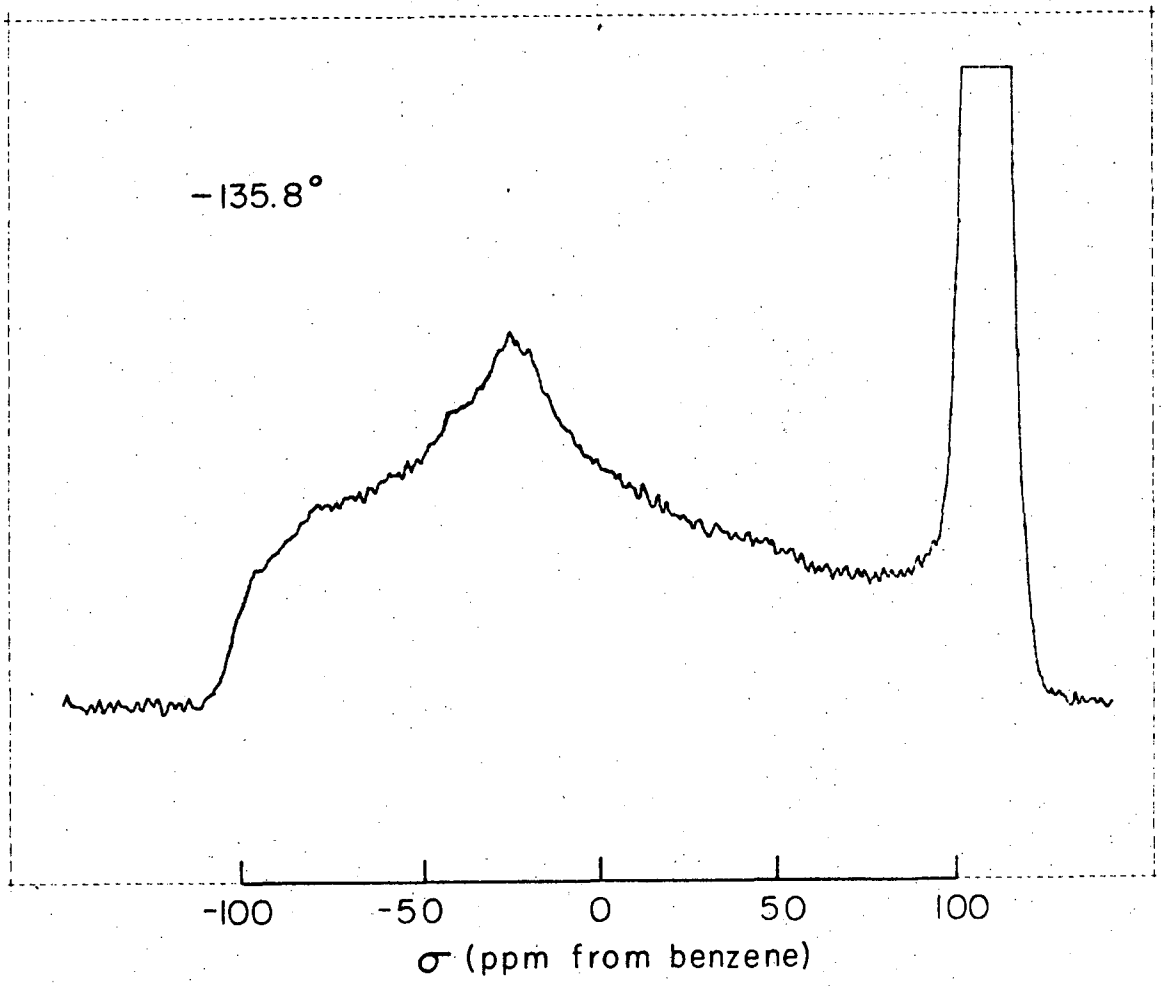

Figure 19(a)

0 0 0 0 4 4 0 6 7 7 0

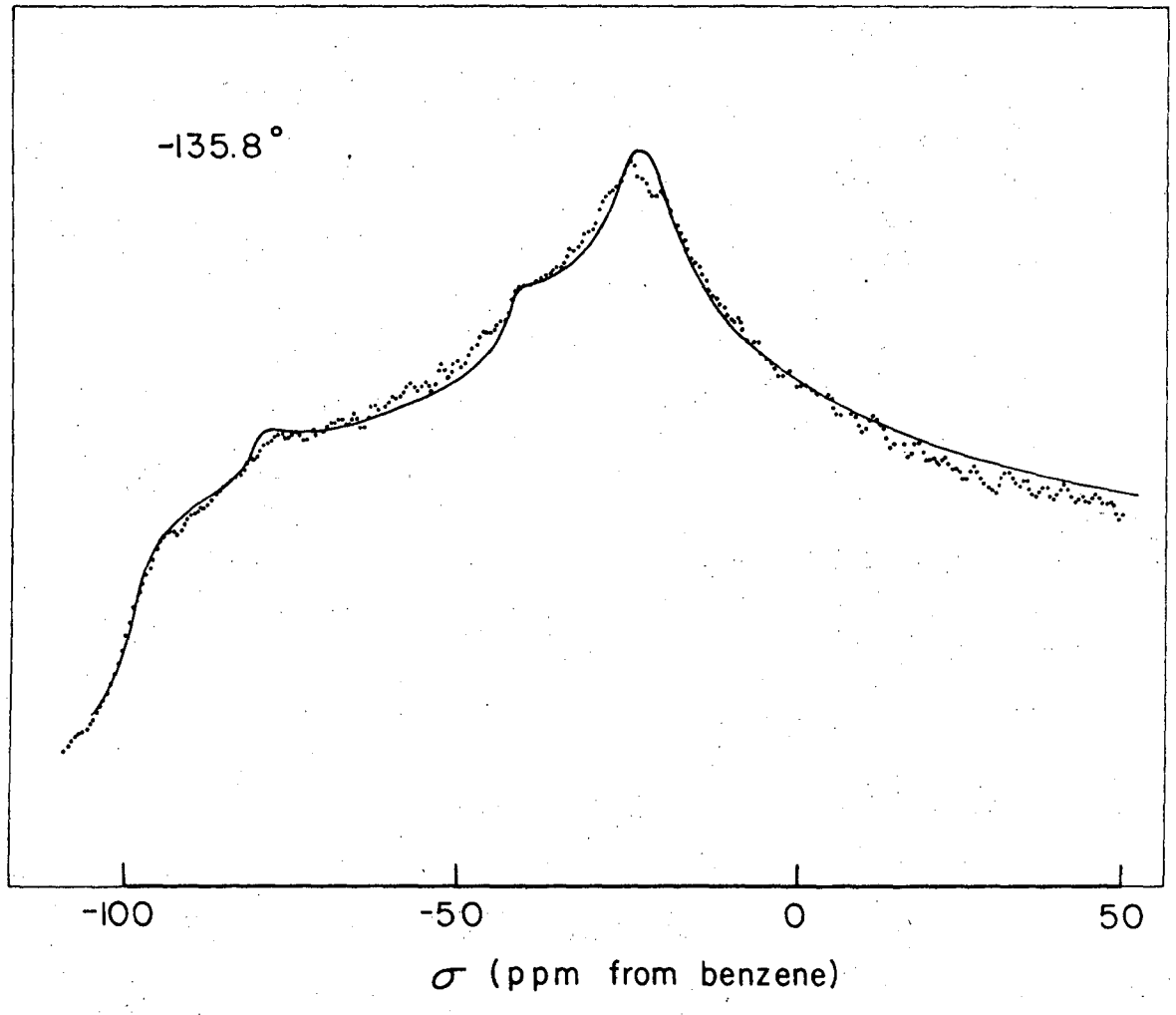

Figure 19(b)

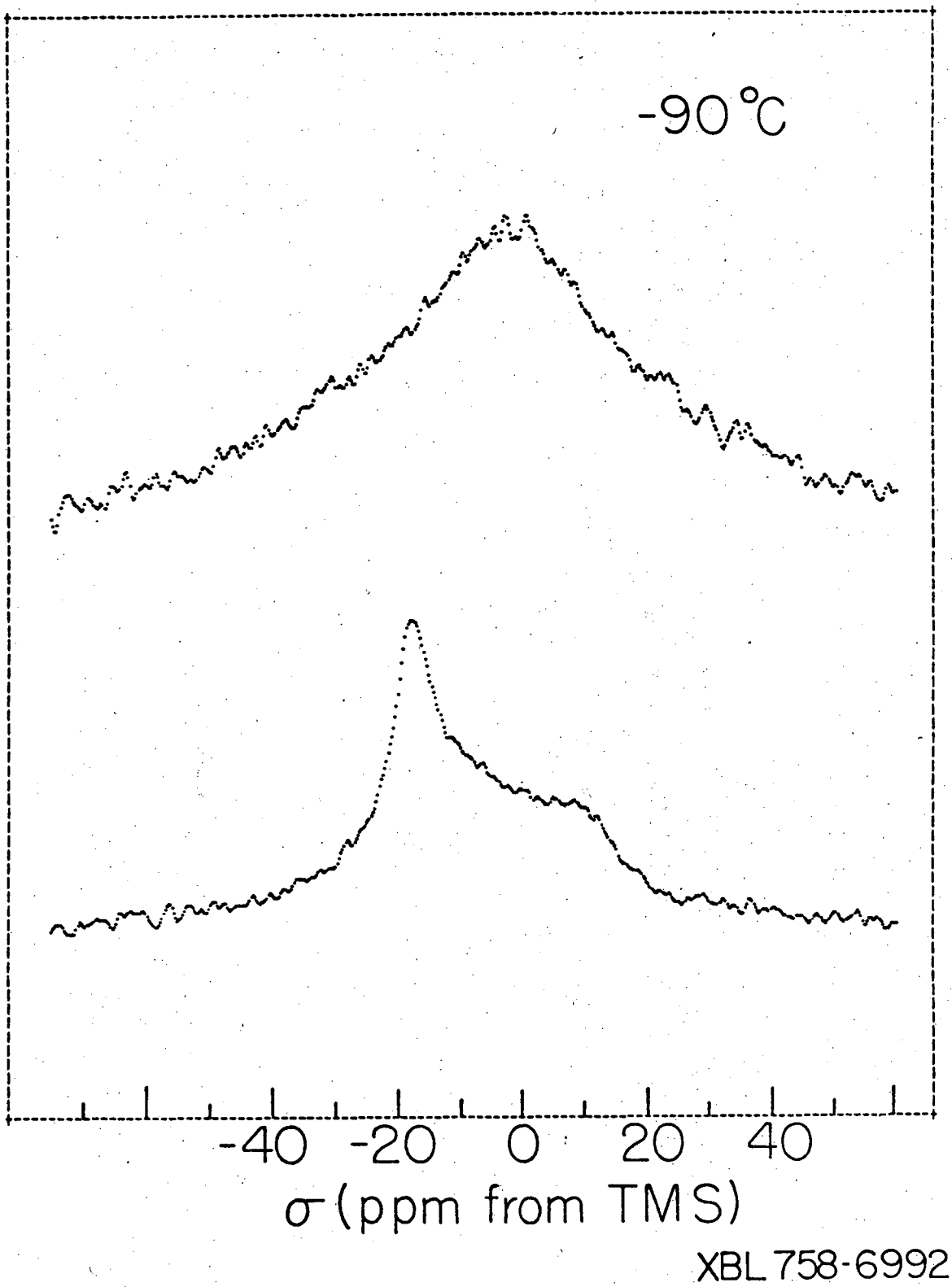

Figure 20

0 0 0 0 4 4 0 6 7 7 1

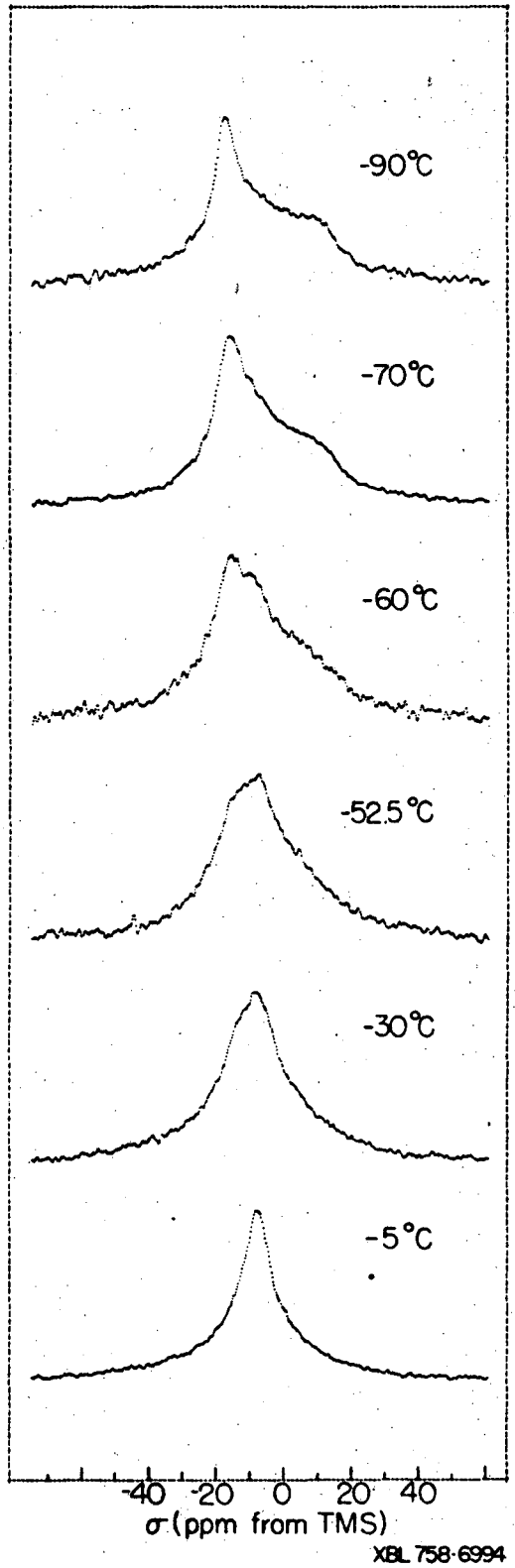

Figure 21

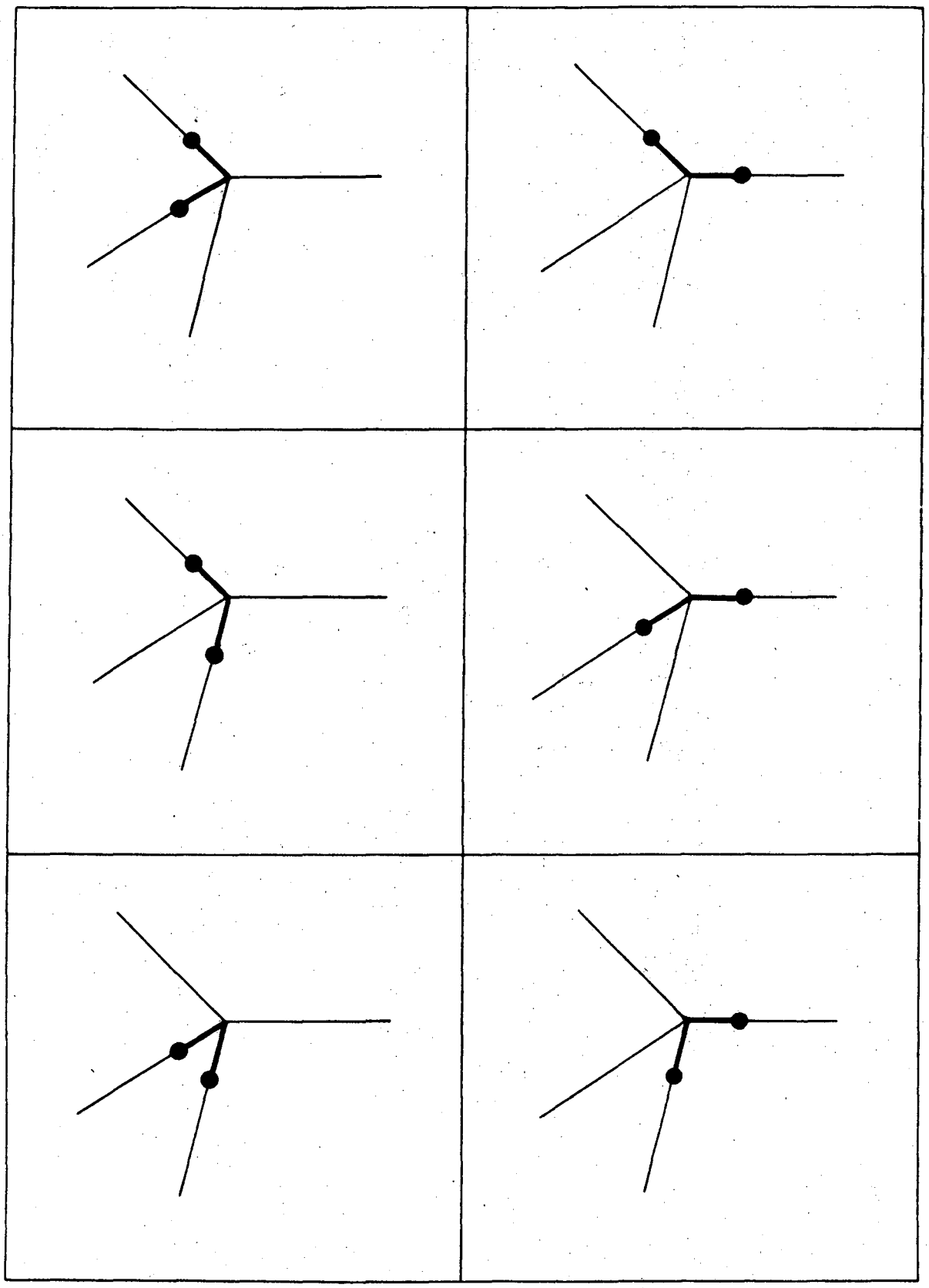

XBL 759-8288

Figure 22

0 0 0 0 4 4 0 0 7 7 2

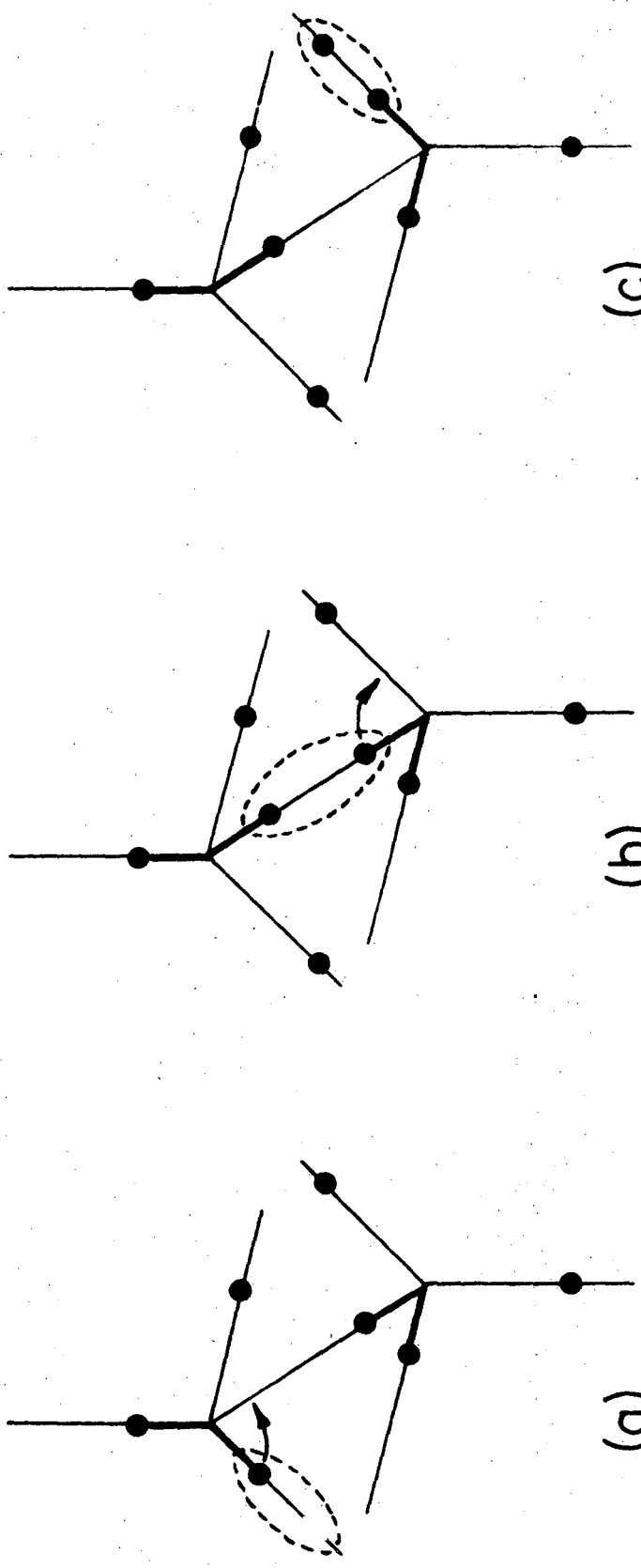

XBL 759-8287

Figure 23

0 0 0 0 4 4 0 0 7 7 3

LEGAL NOTICE

This report was prepared as an account of work sponsored by the United States Government. Neither the United States nor the United States Energy Research and Development Administration, nor any of their employees, nor any of their contractors, subcontractors, or their employees, makes any warranty, express or implied, or assumes any legal liability or responsibility for the accuracy, completeness or usefulness of any information, apparatus, product or process disclosed, or represents that its use would not infringe privately owned rights.

TECHNICAL INFORMATION DIVISION
LAWRENCE BERKELEY LABORATORY
UNIVERSITY OF CALIFORNIA
BERKELEY, CALIFORNIA 94720